FINAL REPORT

TOP CEMENT PULSATION FOR PREVENTION OF FLOW AFTER CEMENTING

Andrew K. Wojtanowicz, John Rogers Smith,
Wojciech M. Manowski, and Joseph Martin
Louisiana State University

Submitted to:

US Department of Interior
Minerals Management Service
381 Elden Street
Herndon, Virginia 20170-4817

Baton Rouge, Louisiana
September 15, 2000

TABLE OF CONTENTS

EXECUTIVE SUMMARY

In the Top Cement Pulsation (TCP) technology, low-frequency pressure pulses (using compressed air or water) are applied to the top of cement in the well's annulus after the top cement plug is bumped and pumping stops. The objectives are to reduce cement slurry thickening and minimize cement transition time in order to prevent migration of formation fluids (gas or water) behind the well's casing.

Several field tests proved the feasibility of this technique and showed that it consistently leads to an improved Cement Bond Log. The objective of this work was to evaluate this technology, verify feasibility of TCP for maintaining transmission of hydrostatic pressure in the cement column and to provide design models and guidelines for application of this technique.

Two theoretical models of pressure pulse propagation in Bingham plastic fluid were formulated and studied. The static mathematical model can predict a change in bottomhole pressure and provide the appropriate amplitude of the pressure pulse. Model calculations showed that a relatively small pressure pulse may restore bottomhole pressure that has been lost due to cement gelation. Also, the restored pressure can be maintained even after the pulse is removed. The wave propagation (dynamic) model calculates attenuation of slurry displacement at depth in the cement column. The results showed that cement rheology and well geometry are the most important factors in controlling pulse propagation. The model also showed that the wave was attenuated the most in small annuli and for slurries with high yield point.

A rheological study, at atmospheric conditions, of the effect of shearing on cement yield point and plastic viscosity indicated that neat cements can be kept in fluid state up to five hours at room temperature. Continuous cement shearing should therefore effectively maintain the high hydrostatic pressure exerted by the cement column. Also, measurements of cement compressibility showed that during the transition time, cement compressibility remains essentially constant implying cement shearing due to pulsation should be feasible during transition.

A concept for a TCP treatment schedule has been developed using two criteria: selective minimization of cement transition time and maintenance of bottomhole pressure overbalance. Selective control of transition time requires varying top pulsation in such a way that at any time the length of the cement section undergoing transition is minimized. During that time, the remaining cement column undergoes pulsation and maintains hydrostatic pressure. The pulsation schedule should also provide pressure pulse amplitudes high enough to maintain bottomhole overbalance even when the whole slurry column is in transition at the same time.

Direct downhole pressure measurements during a field experiment are needed to verify performance of TCP in maintaining pressure transmission in the cement column. Measurement of pressure in an annulus should help accomplish two goals: first, it would show how a pressure pulse is transmitted in setting cement; and, second, it would indicate how pressure-induced cement motion can affect cement gelation by measuring pressure loss caused by this gelation. Achieving the first goal would verify the dynamic model of pressure pulse propagation, while achieving the second would verify the effects of cement rheology on which the models in this study are based. Improved HPHT measurements of cement rheology representative of downhole properties would be needed to be complete this verification. In addition, HPHT measurements of rheology at low shear rates are necessary to identify the minimum shearing necessary to suppress the tendency for the yield point of the slurry to increase.

Given the expense of measuring downhole pressures in a cement column, full-scale tests were conducted at the LSU well facility using “cement-like” fluids to investigate TCP. A slurry of water, bentonite, and polyanionic cellulose was formulated to give a yield stress and early-time gel strengths similar to a cement slurry. The tests with this fluid demonstrated that yield

stress and well geometry are the major influences on transmission of hydrostatic pressure and pressure pulses downhole. Gel strength was shown to have an influence that was similar to, but much less significant than, yield stress on the transmission of hydrostatic pressure. Pulsation was observed to restore downhole pressures more rapidly than application of a constant pressure equal to the pulse amplitude. The frequency and relative duration of pressure pulses also influenced the degree to which pulsation was successful in restoring hydrostatic pressure.

BACKGROUND INFORMATION

Flow after cementing occurs when gas or water from permeable strata invades freshly placed cement and migrates upward in the well's annulus. The phenomenon can create potentially hazardous surface or underground blowouts, loss of well integrity and environmental pollution, or annular leakage and sustained casing pressure, which leads to inability to abandon the well.

Remedial treatment of early flow after cementing by squeeze cementing is feasible but costly. However, late flow after cementing is difficult to correct because it usually occurs in producing wells where casing annuli cannot be circulated. Presently, there are no corrective measures for sustained casing pressure prior to abandoning offshore wells. Therefore, it is critical to focus on preventing annular flow after cementing rather than combating the problem. Moreover, there is no preventive method currently available that would work in all cases.

According to the Minerals Management Service (MMS), a US government agency that manages US Gulf Coast offshore resources, there has been an increasing trend in shallow gas and water flow incidents in the Gulf of Mexico (GOM) over the last decade. This is a result of increased drilling activity in the GOM, especially in deep waters.

The mechanism of flow after cementing has been extensively studied for the past 20 years. A hydrostatic pressure loss after cement placement has been identified as the primary reason for fluid migration outside wells. A well with progressive pressure loss becomes underbalanced, which results in formation fluid entry and migration.

1.1 Hydrostatic Pressure Loss After Cementing

In 1983 a landmark field experiment was performed by Exxon to verify hydrostatic pressure loss in annuli after primary cementing in wells (Cooke, 1982). Shown in Fig.1 is the downhole instrumentation used in these experiments. Six pressure gauges were strapped onto the 2 7/8 in. casing in the 7 7/8 in., 8900 ft well. Then, nearly 400 bbl of 16.6 pg cement slurry was placed in the well's annulus. (The density of drilling mud was 10.2 ppg.) Figure 2 shows a plot of pressure history recorded by the gauges. An exponential pattern of hydrostatic pressure loss is evident in all curves.

Shown in Table 1 are the values of hydrostatic pressure loss recorded by six pressure gauges installed at different depths (see Fig.1). Almost a 3,000 psi pressure loss was observed at the depth of 8,754 ft.

Table 1. Hydrostatic pressure loss in cement column (Cooke, 1982)

Depth (ft)	Pressure at placement (psi)	Pressure 360 min after placement (psi)	Pressure loss (psi)
3,636	2,600	1,700	900
4,632	3,400	2,050	1,350
4,787	3,550	2,300	1,250
5,488	4,200	2,550	1,620
6,909	5,450	3,150	2,300
8,754	7,100	4,150	2,950

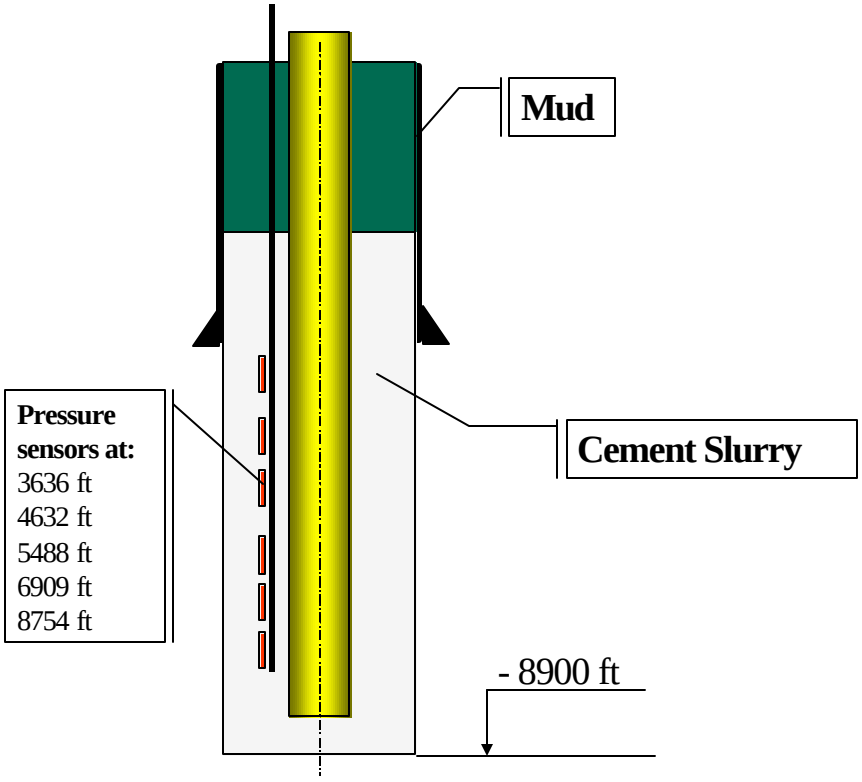

Figure 1. Downhole installation in Exxon experiment (Cooke, 1982)

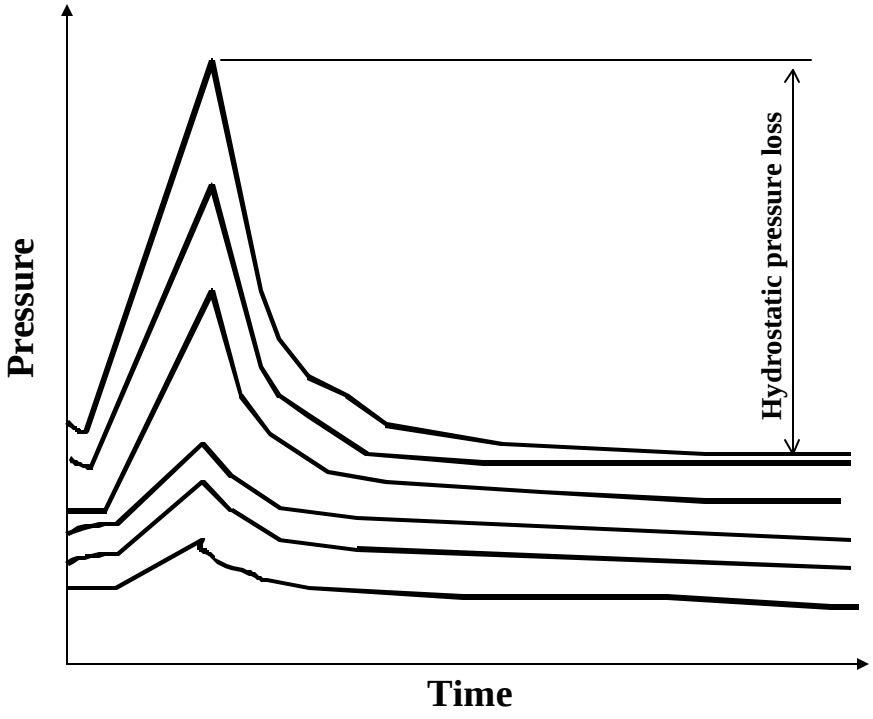

Figure 2. Loss of hydrostatic pressure in annulus after cement placement

2. MECHANICAL METHODS FOR PREVENTION OF FLOW AFTER CEMENTING

Prevention of flow after cementing has been approached in two ways, either by formulating special cement slurries or by using mechanical concepts such as modification of slurry rheology, downhole installations, or placement procedures.

2.1 Mud Displacement

Incomplete mud displacement from a cemented annulus can leave a continuous mud channel which may become a path for a flow of reservoir fluids. Thus, the main objective of cementing, i.e., complete and permanent well isolation, will not be achieved. This is why mud removal should be a topic of high interest for the engineers involved in cementing technology. Mud displacement is a notoriously difficult subject to study both theoretically and experimentally, and a review of the state of the art goes beyond the scope of this work.

A number of mechanical devices are very helpful in removing mud and mud cake. These are: casing centralizers, fluid jets, scrapers and scratchers. Also, casing reciprocation and rotation during cement pumping is very helpful. An essential part of good cementing practices is preparing the borehole. Some key issues are: minimizing doglegs; creating a stabilized, in-gauge hole; treating the mud appropriately so that it is free from cuttings and renders thin, dynamic filter cakes. The displacing fluid is recommended to be in turbulent flow regime, and the annular space should be in contact with the fluid for a sufficient period of time. In order to achieve turbulent flow, the viscosity of the displacing fluid should be kept low, often lower than the mud's viscosity.

Achieving turbulent flow during cement pumping is not always possible, especially in conductor and surface casing operations. For laminar flow conditions, one theoretical and a number of experimental studies involving non-Newtonian fluids have been done to find what conditions control displacement efficiency the most. Generally speaking, density, yield point and viscosity ratio of the displacing fluid to displaced fluid are critical. The displacing fluid is recommended to be at least 2 lb/gal heavier than the displaced fluid. Also, yield point and viscosity ratio should be greater than unity.

2.2 Adjustment of Cement Slurry Column Height

This concept was presented by Levine et al. (1979), in which a graphical technique to predict a potential for annular gas flow was developed. The hydrostatic pressure exerted by the cement column is assumed to drop down only to the water column pressure. It is worth noting that in the light of recent investigations, pore pressure in cement column can drop below that value (suction effect). If this pressure is lower than the pore pressure, the author suggests a number of techniques:

- minimizing the cement column height;
- increasing annular mud density;
- multistage cementing; and
- modifying the cement slurry water density, or thickening, time.

Obvious limitations of the technique of minimizing the cement column height are that a cement needs to be placed against all zones that require isolation and casing must be adequately supported. Also, regulatory requirements must be considered. When the cement column height is lowered, the weight of the annular mud on top of the cement can be increased. However, this technique may not work at all due to the cement's high static gel strength (SGS), which will

prevent the mud hydrostatic pressure from being transmitted. Multistage cementing is not a viable alternative on a routine basis due to its high cost. According to the present status of knowledge on the mechanism of pressure loss in cement slurry, increasing mix water density may not prevent migration of fluids after cementing.

2.3 Application of Annular Back Pressure

This technique was suggested by Levine et al. (1979) and field-tested by Cooke et al. (1982). The concept is simple. Injecting water to the top of the sealed annulus, thereby applying surface pressure, can compensate for the decline of pressure exerted by the cement column. As mentioned above, a clear problem that must be overcome here is cement SGS buildup that may prevent transmission of pressure. Indeed, field measurements confirmed pressure of 60 psi applied about 10 hours after pumping had been completed was not transmitted lower than the depth of 1900 ft below top of cement. However, earlier application of pressure in the order of 60-100 psi appeared to prevent the loss of hydrostatic pressure up to the depth of 4500 ft below the top of the cement column well up to 5 hours after pumping had been completed. Approximately 15 hours after pumping had been completed, an application of 500 psi broke the bond in the column down to 5400 ft (about 4400 ft below the top of the cement column) and caused a surge of more than 1000 psi in recorded downhole pressure. This experiment showed that SGS grows very rapidly in static columns of cement and indeed a high surface pressure would be necessary to break the gel and restore the pressure. Also, it showed that a rapid decline in the restored pressure follows. It was clear that gel strength would rebuild very quickly and this technique turned out not to be effective.

2.4 External Casing Packers

External packers inflate when specific pressure differential is applied onto them. They seal the annulus and therefore prevent upward migration of fluids. These devices cannot be effective against soft formations; this is a severe limitation for most areas in the Gulf of Mexico, where shallow sediments are often poorly consolidated. They were reported to set prematurely and sometimes tend to get damaged while the casing they are attached to is run down the hole. According to some critics, as they are set, they stop transmitting any pressure from above them. Thus, they may trigger or accelerate fluid migration and further exacerbate the problem rather than prevent it.

2.5 Low-Speed Casing Rotation/Reciprocation After Cement Placement

The reasons for casing movement are to improve mud removal and to modify the cement transition time. The movement delays loss of hydrostatic pressure in the cement column. Once casing is not moved any more, cement starts to set very quickly and develops high resistance to deformation so that formation fluids do not have enough time to migrate upward.

Laboratory tests done to develop the technique showed that slow movement of a pipe creates a thin water layer around it. Once movement is over, the layer heals very fast, so the cement can create a bond with the pipe. Fig. 3 presents transition times of a slurry setting under static conditions and the same cement slurry setting while the pipe was moving slowly, after Sutton and Ravi (1991). The latter transition time is much shorter. It was recommended that the casing be either rotated at the rate of 2-8 rpm, or reciprocated at 0.2-2 ft/min depending on the size of the casing. That is, the authors found that the minimum rate to maintain liquidity was between 3 and 7 ft/min for casing rotation and 1.7 ft/min for casing reciprocation. Also, it was found that the torque needed to rotate the casing was much less than torque calculated from SGS.

The observed torque for casing rotation or load for casing reciprocation are within the allowable range for casing thread and hook load, according to the authors. This technique, although sound in principle, has not been used much.

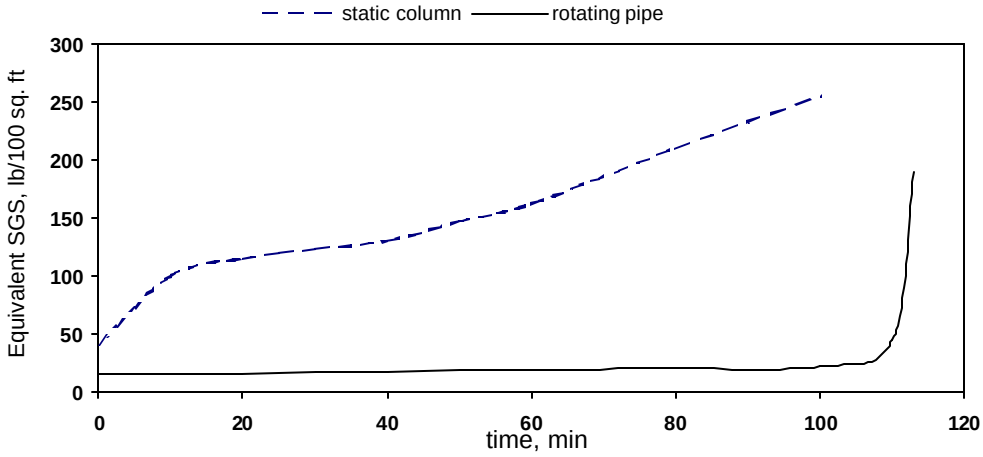

Figure 3. Static vs. rotating column pressure loss, after Sutton & Ravi, 1991

2.6 Casing Vibration

The idea of vibrating the casing while and/or after cement is pumped is to minimize the cement transition time by fluidizing the slurry. Once vibration ceases, the cement should set very quickly. An overview of recent patents employing various methods of vibrating either the casing or the cement slurry directly is presented in Table 2.

Table 2. Review of patents granted in the area of mechanical vibration of cement

Patent granted to:	**Description of the apparatus:**	**Extent of use:**
SOLUM OIL TOOL, 1971, after Solum & Solum (1969)	attached to the drill pipe, when pipe is rotated, it repeatedly strikes against the casing	Used mostly for gravel pack compaction, vibration can be applied only when cement is pumped
EXXON, 1981 after Cooke (1981)	vibration applied after pumping, various methods proposed: hydraulic jars, explosives, adapted geophysical vibrator	Laboratory experiments using oscillatory viscometer as well as a short column filled with cement both confirmed that vibrating results in restoring hydrostatic pressure or delaying the loss of hydrostatic pressure.
EXXON, 1985 after Keller (1985)	oscillation of drilling mud or preflush to remove mud cake and break the gel near the walls	Field tests showed that mud displacement efficiency increased from 65% to 90%.
A. Bodine,	sonic oscillator coupled to the	?

1987 after Bodine & Gregory (1985)	casing collar during cement placement and curing	
R.E. Rankin, 1992 after Rankin (1992)	vibrating element mounted near the bottom, an eccentric element periodically strikes against casing when fluid is pumped through the pipe	It works only during slurry pumping.
EXXON, 1992 after Winbow (1992)	application of pressure pulses to liquid-filled casing interior after cement placement	?
J. Haberman, Texaco, 1995 after Haberman, et al. (1993)	application of pressure pulses to the annulus after cement pumping	Field tested, preliminary results show better CBL; The technique is feasible.

A series of laboratory experiments (Chow et al., 1988) that involved a cement sample subjected to oscillatory deformations showed that amplitude of about 0.001 in. was enough to minimize the elastic modulus of the slurry. The frequency of the oscillations was found to have relatively little effect on the value of the elastic modulus. The frequency was, however, in the range of 20 Hz. The laboratory procedure simulated wellbore geometry: two pipes were placed concentrically, and an electromagnetic driver capable of vibrating was attached to the inner pipe.

The effects of driver frequency and amplitude on the pressure near the bottom of the annulus were recorded. It was found that, after 90 min. of waiting, amplitude of 0.015 in. was enough to restore the pressure to its original value. Frequencies in the lower range of the instrument appeared to be more effective. A visual observation revealed that a thin layer of liquefied cement was created near the vibrated pipe, much like in the case of low-rate pipe movement.

A field experiment using a 200 ft long casing string was then carried out. Pressure transducers and accelerometers were attached to the casing and run. A geophysical truck capable of vibrating the casing was used. Vibration of the casing was successful in restoring hydrostatic pressure up to 230 min. when the response was getting very slow. The results of the experiment showed that a frequency of 8 Hz was optimal. A temperature rise signaling the end of the dormant period of the cement began at 150 min. There was a strong correlation observed between this time and the time when hydrostatic pressure of the cement began to drop significantly. It indicates that the pressure loss in cement columns is affected mostly by hydration of cements. Cement slurry vibration has been shown to be an effective method of preventing the loss of hydrostatic pressure. It has not been used in the field since the tests. Apparently, all the heavy equipment needed to vibrate a long and heavy string of casing renders the method not feasible, even onshore.

3. TOP CEMENT PULSATION (TCP) METHOD

This method is an extension of the application of annular pressure at the top of the cement column. Instead of applying constant pressure, pressure pulses are applied to the top of the sealed annulus. The objective is to maintain the cement slurry in a fluid state so that hydrostatic

pressure would not decline. Once the pulsations are ended, the slurry will develop a structure highly resistant to any deformation. This will minimize the slurry transition time. Another potential benefit from this technology is an improved Cement Bond Log (CBL) (Haberman, 1996). The equipment used to reciprocate the slurry is very simple and inexpensive. Fig. 4 shows a schematic of the assembly used.

The equipment used consists of an air/water compressor and a back pressure valve. Air or water is compressed and injected into the closed annulus within 5 seconds. When the pressure reaches 100 psi, the back pressure valve is opened and air/water is exhausted. The exhaust cycle takes about 5 seconds, and the full cycle is about 10 seconds. During the compression cycle, the column of cement will travel downward due to the compressibility of the cement slurry and expansion of the borehole as well as the compression of the casing. The contribution from the casing may be neglected due to the small pressure applied.

CBL logs for cemented wells where TCP was applied indicated consistently a better bond as compared with those where cement was set undisturbed. With this technique, the fluidity of the slurry is monitored by periodically measuring the volume of water or gas pumped into the annulus to increase the pressure to 100 psi. Compressibilities of the system obtained in such a way turned out to be 2 to 3 times greater than the compressibility of water for a given annulus. The change of compressibility due to cement setting determined by the observation of the volume of fluid pumped into the annulus is shown in Fig. 5. A relatively short thickening time most likely caused by slurry dehydration was noted as the cause of the rapid decline of the system compressibility. There are, however, other possible mechanisms: attenuation of the pressure wave by the thickening cement slurry; decline of cement compressibility due to its thickening; and the cement slurry's inability to transmit horizontal stresses effectively due to its plasticity.

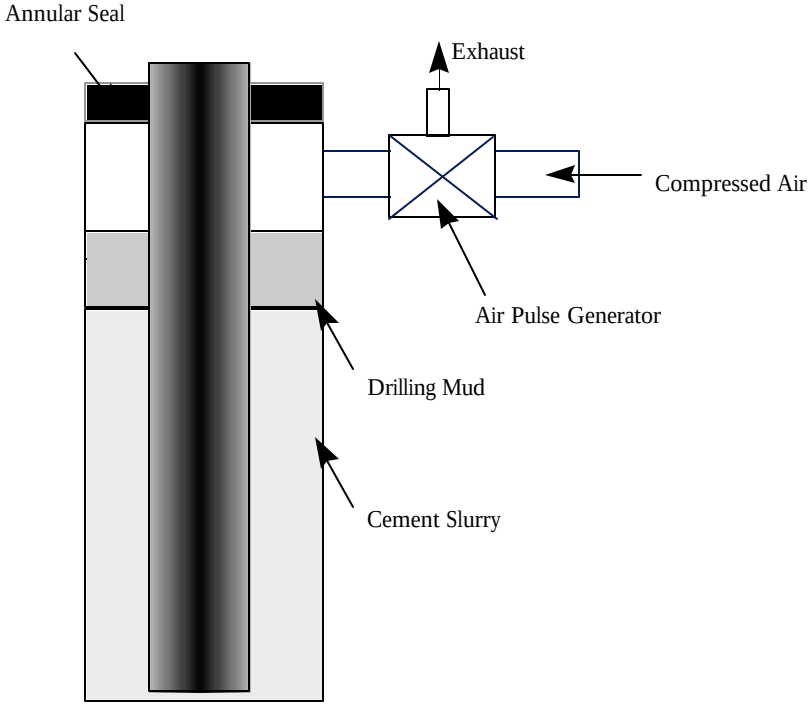

Figure 4. Schematic of equipment used in TCP

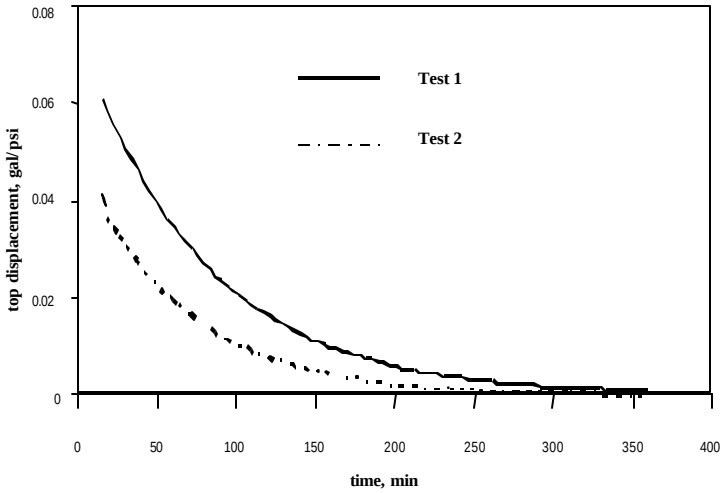

Figure 5. Top cement amplitude change during TCP treatment of shallow wells in Permian Basin (Haberman, 1997)

3.1 Comparison to Other Cement Vibration Concepts

Cement vibration using a low-frequency cyclic pulsation has become a well established method in the construction industry for improving the quality of cement. This quality has been related to better compaction, compressive strength, and fill-up. Cement gelation or transmission of hydrostatic pressure has not been a concern in these applications.

In the oil industry, "vibrating" cement in wellbore annuli was initially considered to be a *method for manipulating the casing string* in order to keep cement slurry in motion through casing rotation or reciprocation (Carter and Slagle, 1970; Carter et al., 1973; and Christian et al., 1975). The motion would improve displacement of drilling mud and placement of cement slurry in the annulus. Similarly, enhanced filling of the annulus with cement slurry ("compactly placing...without rotating or reciprocating the casing") was considered the main advantage of the first casing vibration method with mechanical vibrator placed at the bottom of casing string (Solum et al., 1971).

Using forced casing vibrations for early gas migration control has become the subject of several inventions over the past seventeen years (Cooke, 1983; Keller, 1985; Bodine, 1987; Rankin, 1992; and Winbow, 1994). Despite various types of vibration generators proposed in these inventions, the very concept of gas migration control was the same. It was based upon experimental observations that cement slurries in continuous motion remained liquidous for longer periods of time than did a still cement slurry. These observations have been supported by the following findings (Cooke, 1988):

- During hammering at a steel pipe submerged in cement, the observation was made that a concentric layer of slurry around the pipe remained in liquid state and could flow while the outer slurry became gelled;
- When a low-frequency (8 cycles/sec) vibrations were applied to the casing string surrounded by cement slurry in a 200 ft well bottomhole hydrostatic pressure was almost instantly (2-3 sec) restored as shown in Fig. 6;
- Casing vibration caused instant compaction of the cement column, shown in Fig. 7, which indicated that void spaces were most likely present in the dormant slurry (i.e., building of structure and transition from liquid to semi-solid).

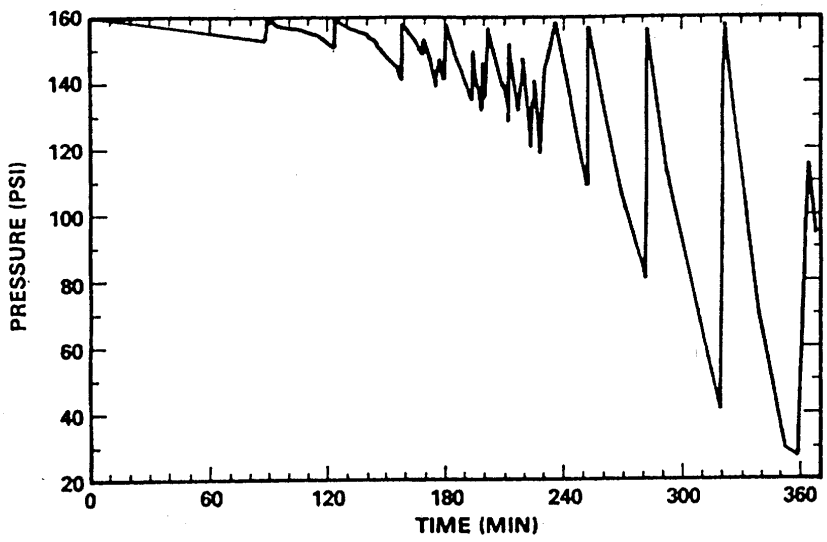

Figure 6. Restoration of bottomhole pressure due casing vibration (Cooke, 1988)

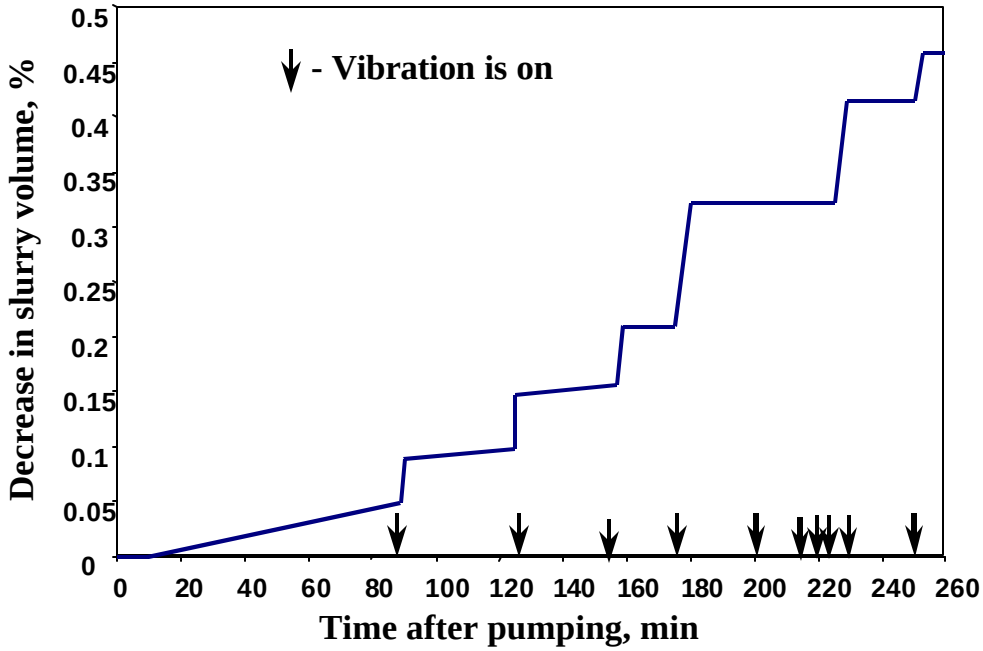

Figure 7. Liquification of cement slurry in response to vibration measured as an instant drop of slurry level in the annulus (Coke, 1988)

Using the casing to keep cement in motion has one fundamental disadvantage: it provides the same level of vibration at various depths to the cement slurry which is at various stages of the setting process. The rate of slurry setting is a temperature-controlled process of hydration (Schlumberger, 1990) and the annular cement usually starts to set from the bottom up, thus following the wellbore temperature distribution. (The temperature distribution may not be uniform, with the maximum temperature being at about one-third of the well's depth from the bottom [Raymond, 1969]). The uniformly distributed vibration may liquify cement in the upper annulus while damaging the bonding between cement and casing and creating a microannulus in the bottom annulus. The TCP technology, on the other hand, imposes motion to cement slurry

directly at the slurry top without using casing. Moreover, the downward propagation of the pressure wave is limited by structural strength of the slurry which means that TCP would *selectively fluidize* only the upper section of the cement column, being at an early stage of gellation, while leaving the bottom and set cement unaffected.

3.2 Physical Mechanism of TCP

The physical mechanism underlying the cement pulsation concept can be explained by examining the phenomenon of the top pressure pulse amplification with depth and possible source of potential energy storage in the cement. The effect was observed in the field tests when a 400 psi constant pressure load was applied to the top of cement in a 6000 ft well (Sabins et al., 1988). The resulting increase of pressure at depth was greater than 400 psi and showed an increasing trend with depth up to over 1000 psi, as depicted in Fig. 8. A similar response was observed when a single cycle of pressure with 60 psi amplitude was applied to the cement slurry in a 300 ft well (Haberman, 1996). The pressure signal was amplified to almost 100 psi at the well's bottom, and the trend was consistent with depth, as shown in Fig. 9.

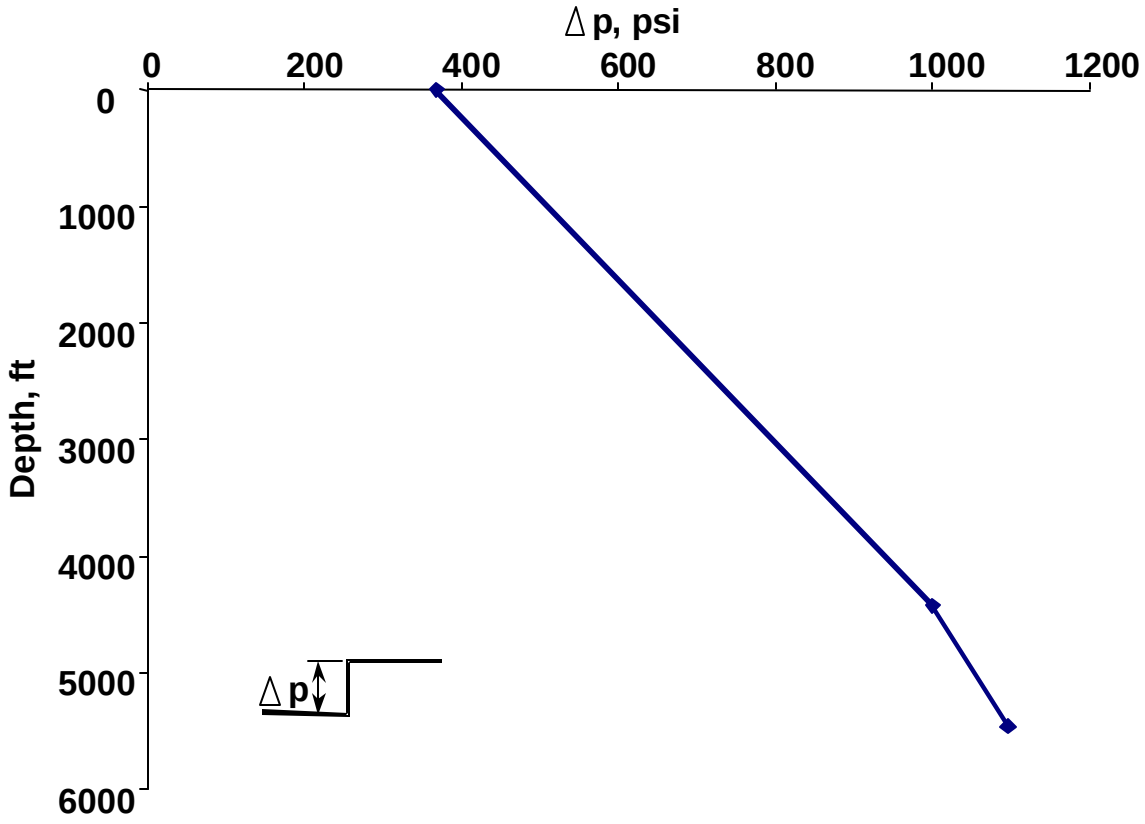

Figure 8. Step pressure increase at cement top is amplified at depth (Haberman, 1996)

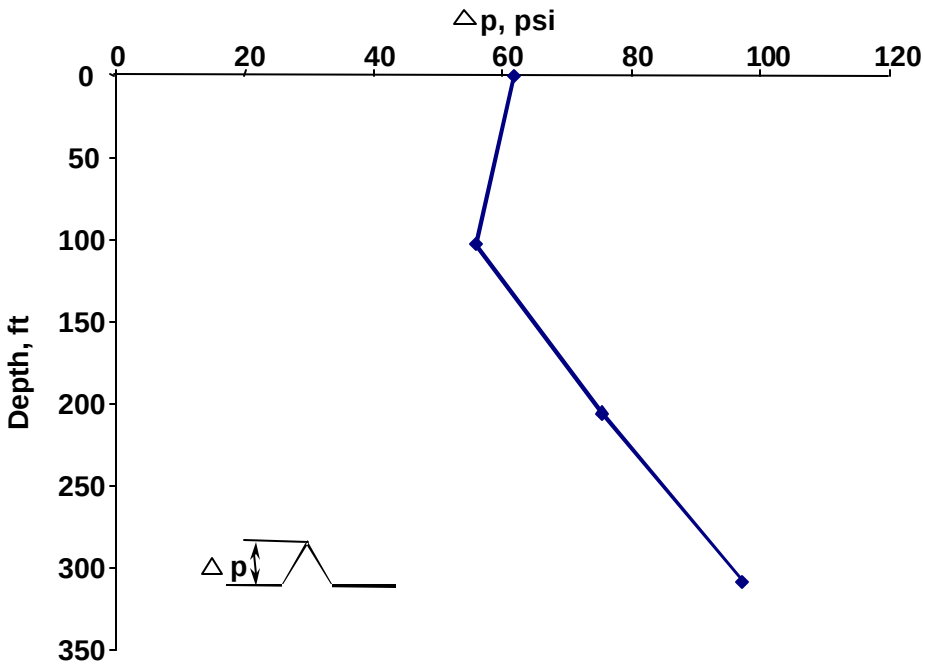

Figure 9. Top pressure cycle with 62 psi amplitude is amplified at depth (Haberman, 1996)

The amplification of pressure signals with increasing depth is attributed to the stored potential energy resulting from the fact that part of the hydrostatic pressure is supported by progressive gel strength. The development of static gel strength is well documented in the cementing literature for different types of cement slurries as shown in Fig. 10. It has also been documented experimentally that using low shearing rates, as shown in Fig. 11, can alter the development of gel strength. This analysis, together with the results depicted in Fig. 6, indicate that when shear is applied the slurry will respond by reducing its resistance to flow from the upper curve, shown in Fig. 11 (Static Gel Strength) to the lower curve (Yield Point). Thus, the physical mechanism active in cement pulsation results from the thixotropic property of cement slurries.

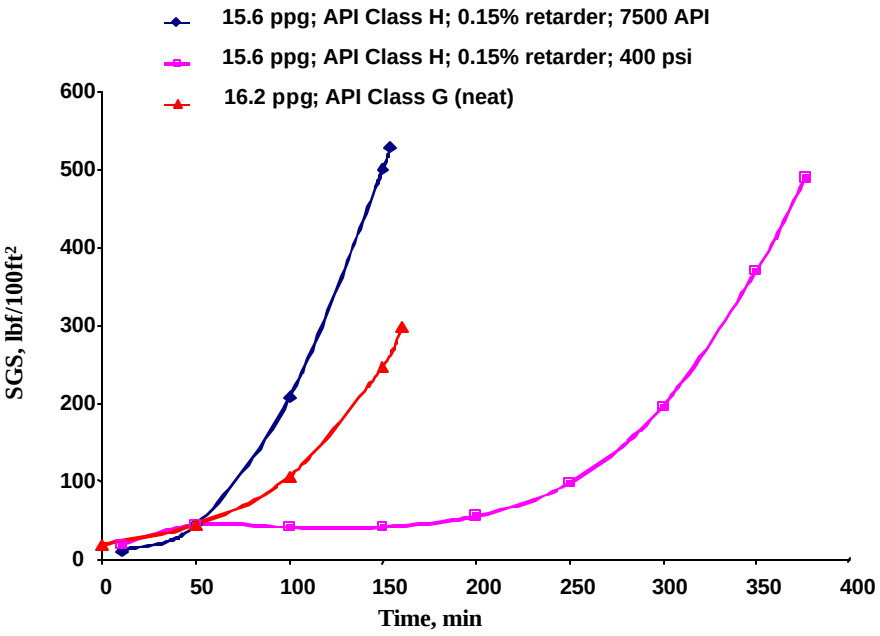

Figure 10. Development of static gel strength in time for various cement slurries (Sabins et al., 1988; Sutton et al., 1989)

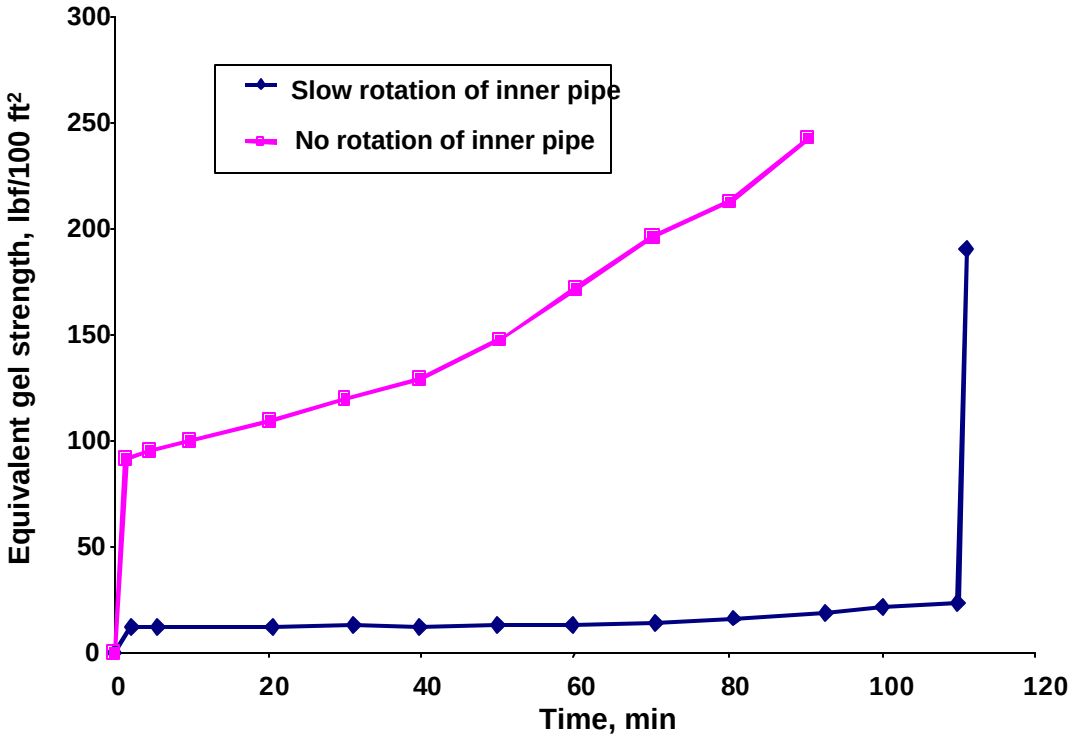

Figure 11. Two levels of cement slurry gelation: without shear (upper plot), and with shear (bottom plot) (Sutton et. al., 1991)

3.2.1 Shear-Induced Structural Breakup of Cement Slurries

Our conceptual model of the cement pulsation technology draws from the low-shear rate rheology of cement slurries. Within the low shearing rate range, the slurry response reveals both

thixotropic and viscoelastic behavior. Experiments with an oscillatory rheometer (Sutton, 1991) showed that the cement slurry rapidly builds up a basic, solid-like structure (thixotropy) that is resistant to small shearing rates (10 μm amplitude at 10 Hz frequency), as shown by the left curve in Fig. 12. This structure can be broken down, however, with a sufficient value of shearing rate (1000 μm amplitude at 10 Hz) for a 30-second period of time (viscoelasticity). Also, the structure rebuilds in a few minutes even if low-level shear is continued.

Structural breakup of cement slurries has also been documented as a hysteresis of the shear stress v.s. shear rate plots recorded with coaxial viscometers (Banfill, 1981, and Banfill and Saunders, 1981), shown in Fig. 13. In this research the hysteresis loops were attributed to the breakdown of the microstructure (shear thinning) and its re-establishment (shear thickening). Therefore, it can be concluded that during setting time the slurry's flow resistance may assume two different values (upper and lower) for the same value of shear rate. Specifically, at zero shear rate the upper value of stress required to break the slurry's structure can be approximated with static gel strength, while the lower value of stress can be approximated with yield point. These findings support mathematical modeling of cement pulsation.

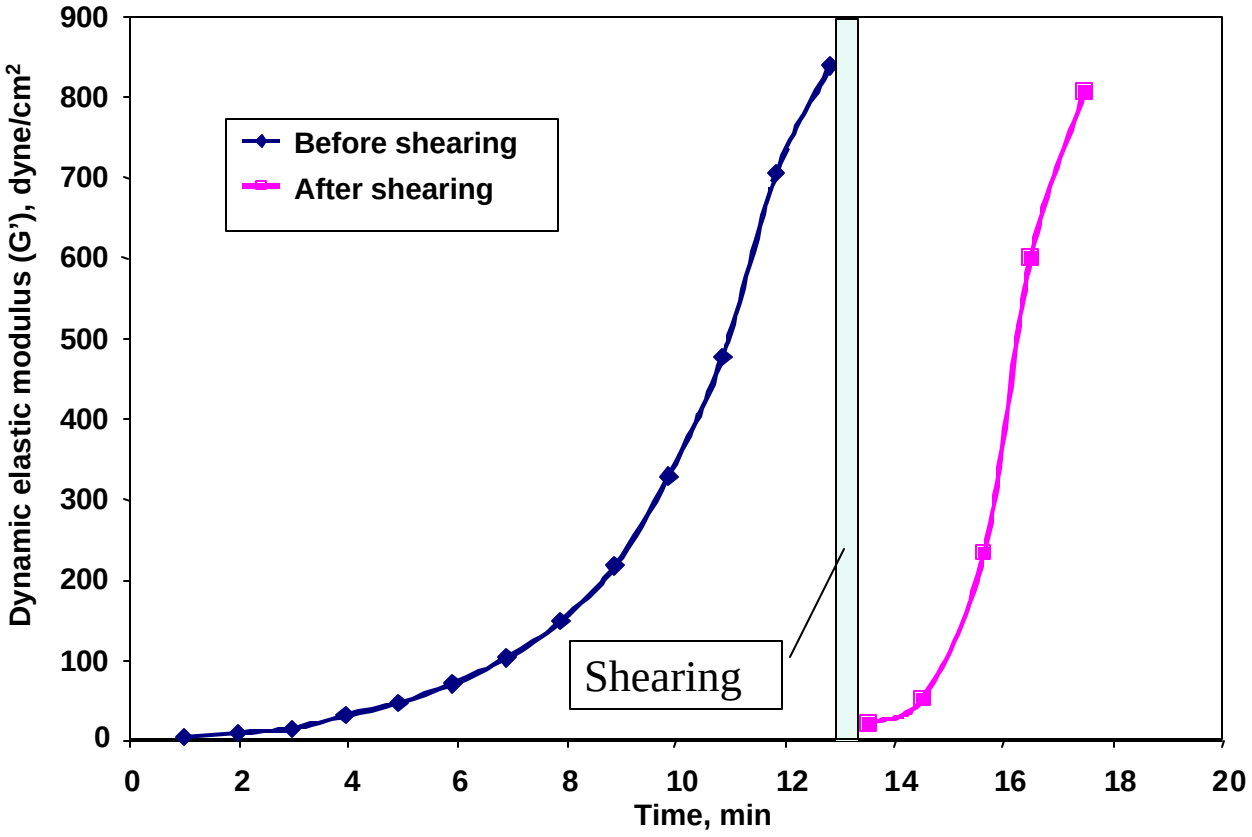

Figure 12. Breakup and rebuilding of cement slurry structure in response to 30-second application of shear rate (Chou et al., 1988)

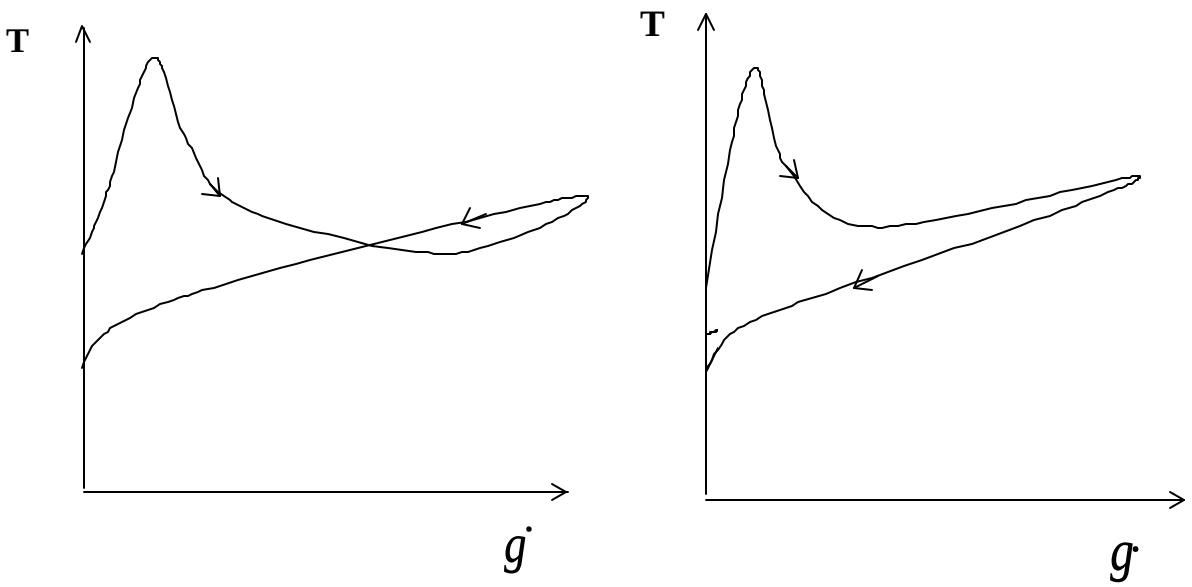

Figure 13. Gel strength and yield point values in cement rheology hysteresis loops (Banfill, 1981, and Banfill and Saunders, 1981)

4. CEMENT SLURRY PROPERTIES RELATED TO TCP

4.1 Compressibility

Since cement compressibility controls both displacement amplitude and wave propagation characteristics, finding how it changes in time is desirable. Specifically, what is the effect of chemical hydration on cement compressibility? The relationship between cement compressibility and wave propagation velocity (Streeter & Wylie, 1967) is:

$$s = \sqrt{\frac{E_{R/C}}{r \cdot c_c \cdot E_{R/C} + 2r \cdot (1+n)}} \tag{1}$$

Equation 1 is valid for an elastic wall forming a circular tunnel. Elastic modulus in this equation represents the effective elasticity of the borehole and casing.

Measurements of cement compressibility were conducted using a high pressure stainless steel vessel. Mercury was injected at controlled volume and pressure. A schematic of the equipment used is presented in Fig. 14. The procedure used was as follows: Cement slurry was mixed according to API Specification 10 and de-aerated using a vacuum pump. Then it was poured into the vessel, and a mercury line was attached to the bottom connector of the vessel. With the top valve open, mercury was slowly injected from the bottom in order to displace all air trapped at the top. When the air-free cement slurry was flowing over the top valve, the mercury pump was stopped and the top valve was closed. Then mercury was slowly injected into the vessel. The volume of the injected mercury and the mercury pressure were recorded.

Fig. 15 presents the combined results of cement compressibility measurements for the case of retarded class H cement slurry. Note the high compressibility at low pressures. This is probably caused by air trapped within the cement slurry despite using the vacuum pump to de-aerate the slurry.

The plots in Fig. 15 show little change in the cement compressibility over the test period. The result implies that the compressibility of the products of chemical reactions is of the same magnitude as the compressibility of the components. Thus, we conclude that during the transition

time, cement compressibility remains a constant component of the annular compressibility of the wellbore.

Assuming that rock mechanical properties and cement density are constant, propagation velocity of the traveling wave can be considered as independent of cement slurry properties. Note that this velocity will not be constant, however, in the whole annulus. In the cased portion of the annulus propagation velocity will be considerably greater than in the open hole annulus. Also, if the open hole section is built of different rocks having different mechanical properties, this acoustic velocity will vary.

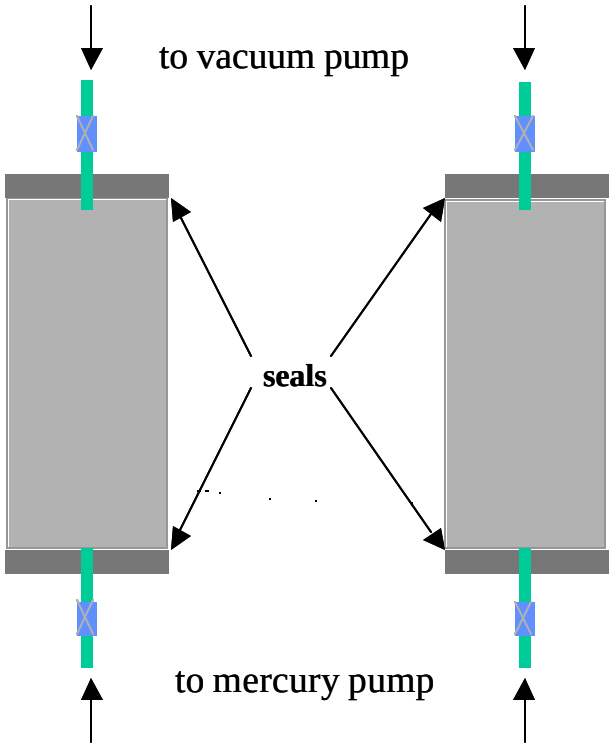

Figure 14. Cement compressibility test cell

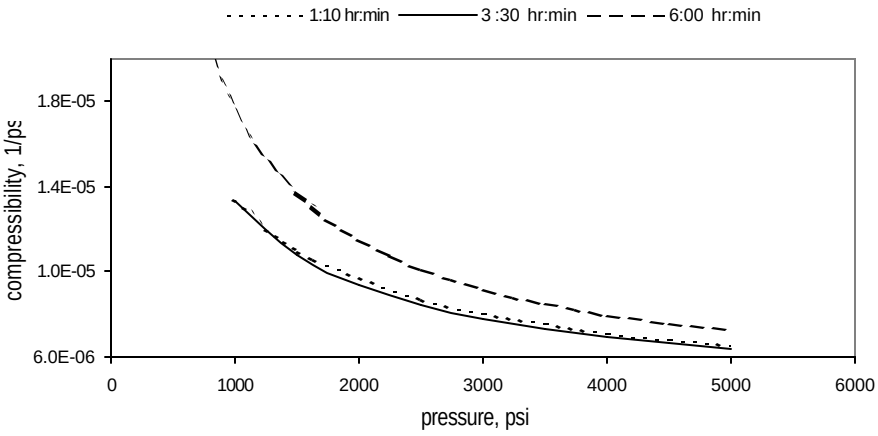

Figure 15. Retarded cement class H compressibility change with pressure and time

4.2 Cement Rheology Under Continuous Shear

Neat class H oilwell cement slurry at room temperature and cement used in an actual TCP field operation were tested. The experiments were conducted in the following manner: Cement was first mixed according to API Specification 10. Next, its density was measured using a pressurized mud balance. Then cement was poured into the cup and continuously sheared using a Fann 35 viscometer. Two sets of tests were performed. In the first set, the rheology of cements used in an actual wellbore was evaluated. In the second, neat cement properties were measured. Since in wellbore conditions cement is subjected to oscillatory shear, and the Fann 35 viscometer is capable of providing steady shear only, a procedure of converting oscillatory shear into an equivalent steady shear was used. The governing equation (Manowski, 1997) is:

$$\bar{v} = \frac{p}{T} \cdot y \qquad (2)$$

For the Bingham plastic fluid, shear rate at the wall (Bourgoyne et al., 1991, p. 144) is:

$$\dot{g}_w = \frac{6 \cdot \bar{v}}{r_2 - r_1} + \frac{1}{2} \cdot \frac{t_y}{m_p} \qquad (3)$$

Combining eq. 2 with eq. 3, yields:

$$\dot{g}_w = \frac{12.0}{T} \cdot \frac{p \cdot y}{r_2 - r_1} + 3.0 \cdot \frac{t_y}{m_p} \qquad (4)$$

Equation 4 relates displacement at any depth to constant shearing rate. A procedure for finding displacement amplitude for any depth will be presented later. This discussion will focus on the results of the rheological tests. Fig. 16 shows yield point development for a sheared (dotted line) and unsheared (solid line) neat cement sample. It shows that up to about 4 hours, continuous shearing can be a method of maintaining high fluidity of neat class H cement at room temperature. Note that in unsheared cement static gel strength starts to build up rapidly after about 90 minutes.

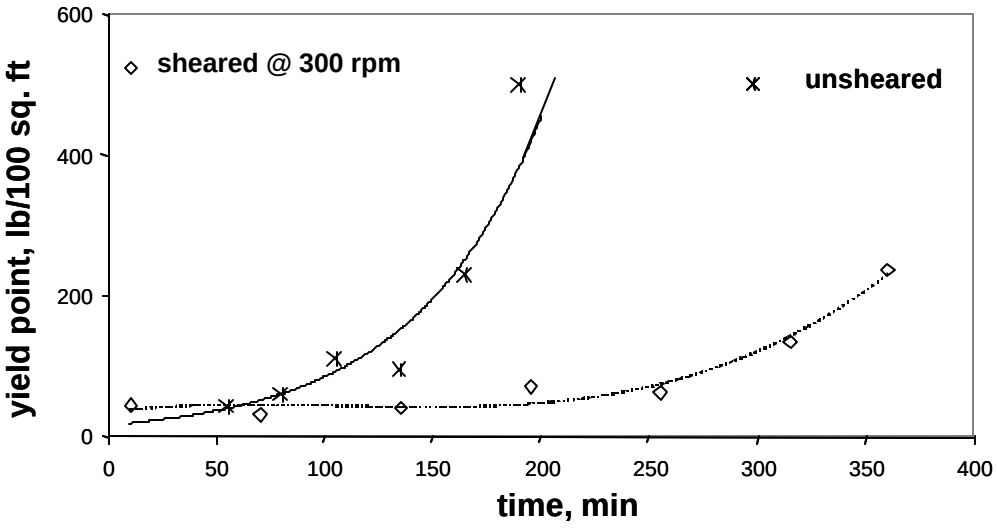

Figure 16. Effect of shearing on development of Yield Point for cement Class H

The experiments also showed that continuous shearing at 3 rpm, the lowest speed available with the Fann 35 viscometer, was enough to maintain the liquidity of the cement sample. Therefore, in this work shearing rate equivalent to 3 rpm was chosen as the minimum

shearing rate to maintain liquidity of cement. This shearing rate did not appear to be a function of time and reached values between 57 and 116 s^{-1} depending on the plastic viscosity and yield point values of cement.

It was then concluded that as low a shearing rate as 116 s^{-1} may be enough to prevent gelation of setting cement and thus maintain high hydrostatic pressure of the cement column. Rheological tests that produce both yield point and plastic viscosity development in time can provide a basis for the design of TCP operation such that only the upper section of cement in the annulus is liquefied while the bottom section remains unsheared and sets rapidly. However, the design of such a "selective" pulsation requires mathematical modeling.

5. TCP MODELING AND DESIGN CONCEPTS

As shown above, field pilot testing of the TCP technology in a 300 ft well using individual pressure pulses showed *increase of the pulse amplitudes with increasing depth.* The observation indicated that propagation of the pressure pulse was controlled by an amplification mechanism which was stronger than the mechanism of pulse attenuation. The only possible source of pressure pulse amplification can be attributed to potential energy stored in the cement column in the process of cement gelation. The propagating pressure pulse releases this energy. However, the energy release is limited and dependent upon depth and size of the initial pressure pulse. On the other hand, strong and very frequent pulses may destabilize the borehole. Therefore, in order to design this technology, a mathematical model needed to be developed describing a relationship between parameters of pulse initiation, amplification and attenuation as a function of depth.

A study has been undertaken at LSU to support the cement pulsation technology with theoretical background and analytical tools. The objectives of the first stage of the study was as follows:

- Compare the cement pulsation with conventional cement vibration methods and explain its unique mechanism;
- Review the research data on cements and define properties underlying the technology;
- Define critical parameters for the treatment design in a particular well; and
- Develop mathematical model describing restoration of bottomhole pressure due pulsation.

5.1 Static Model for TCP Design

The concept of a static model is derived from field results showing amplification of a single pressure signal applied at the top of the cement column instead of the intuitively expected attenuation of this signal with increasing depth.

The amplification of the pressure signal can be attributed to the rapid breakage of gel strength and release of potential energy (hydrostatic pressure loss) stored in the cement column. The energy storage results from the downward movement of the cement column being opposed by development of gel strength. The movement occurs due to volumetric loss taking place in the column (water loss and internal shrinkage). It is postulated that upon the application of shearing, the static value of the yield point of the slurry is reduced to its dynamic equivalent. The static yield point (SGS) represents the maximum value of the shear stress occurring shortly before the static structure is broken. Dynamic yield point (YP), on the other hand, represents the shear stress that must be overcome to initiate flow well after the structure has been sheared.

The reduction from static to dynamic yield point can be a source of partial restoration of hydrostatic pressure in the column, the extent of which will be a function of the difference

between the two yield points (see Fig. 17). The following assumptions are made to derive the static model:

- Time-related values of SGS (static yield point) and YP (dynamic yield point) are known from rheology tests.
- Slurry behaves as a perfect plastic body within the strains occurring in the wellbore and the shape of the stress vs. shear strain curve of the model is shown in Fig.17; shear stress is equal either to the dynamic yield point (YP) or the static yield point (SGS) over the whole range of deformations.
- Slurry is homogeneous throughout the annulus.
- Duration of the pressure load applied to the top is substantially longer than the duration of transient effects; wave phenomena are not taken into account.
- Density variations due to cement compressibility are neglected.
- There is an instantaneous reduction of SGS to YP - a dynamic equivalent of SGS.

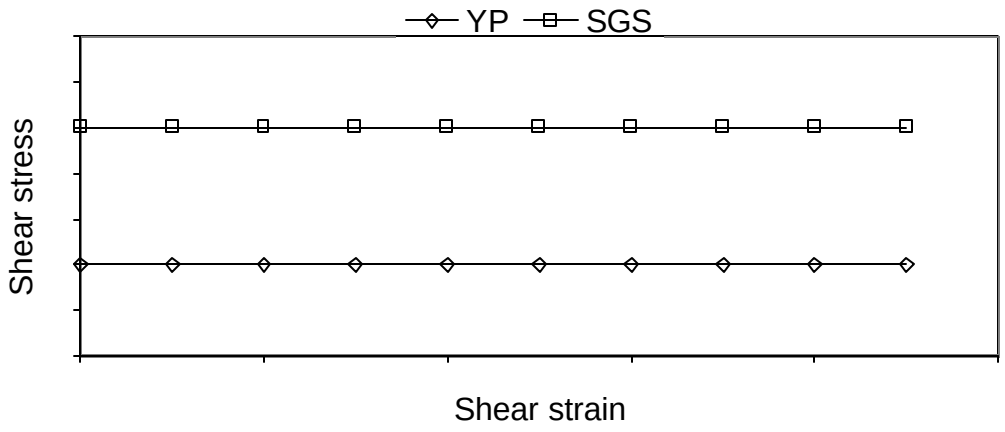

Figure 17. Perfect plastic model of cement slurry

The last two assumptions require a few comments. Since there is only 100 psi applied at the top, the unit volume of cement slurry cannot be compressed substantially. It is especially true in the lower portion of the well where it is already pressurized and its compressibility is very small, thus density variations can be neglected.

The model considers the reduction of SGS to YP an instant phenomenon. The reason is that in this solution we are looking at the ultimate effects of the application of the pulses rather than any transient stages. In reality it takes some time of constant shearing to significantly lower the SGS of the cement slurry. That time will depend strongly on the amplitude and method of deformation. For example, it took roughly 30 sec to liquefy cement slurry subjected to oscillatory motion (10 Hz frequency, 50 μm amplitude) (Chow et al., 1988) while a few minutes were necessary to break the structure in a rotational viscometer where deformations are much larger (Nonat, 1992). There could be two reasons for this behavior. First, oscillatory motion could be much more effective in liquefying cement (frequent change of direction of motion) than steady motion. The deformation of 50 μm appears to be enough to break the gel and higher deformations are not necessary (Chow et al., 1988). Second, the gap in the rotational viscometer (usually not less than 2 mm) is wider than in the oscillatory one (1 mm). It appears that it takes

some time to transfer the "fluidity" from the layer directly subjected to deformations by the rotating element to the layer being in contact with the measuring element.

The third assumption of neglecting transient effects can be justified by comparing the time necessary for the pressure wave to reach the bottom to the frequency of pressure pulses. For average sound velocity in a 3500 ft cement column, it takes 1 to 3 seconds for the wave to reach the bottom of a typical well while the pressure pulse frequency is 0.1 Hz (i.e., by the time cement slurry is pressurized to 100 psi on the top, front of the wave is already on the bottom).

To derive the model, we consider balance of forces describing motion of any cross section of the cement column in the well's annulus as follows:

Pressure gradient (up) - Fluid weight (down) - Wall stress (up) - Inertial force (up) = 0

or,

$$-\delta p/\delta z + g\ \rho(p) - \delta p_f/\delta z - \rho\,\delta^2 u_z/\delta t^2 = 0 \qquad (5)$$

where:
p = pressure
z = depth
g = acceleration of gravity
p_f = pressure opposing slurry motion
t = time
u_z = vertical displacement
ρ = density

Neglecting transient effects and relating pressure to initiate flow, p_f to plastic limit Y yields the following expression:

$$dp = (g\,\rho - 4Y/\Delta D)\,dz \qquad (6)$$

where:
Y = plastic limit, or yield point
ΔD = difference of annular diameters
From the definition of compressibility, density can be expressed as the following function of pressure:

$$\rho = \rho_o\, e^{c(p - p_0)} = \rho_o\, e^{c\,\Delta p} \qquad (7)$$

Pressure as a function of depth may be expressed in differential form as follows:

$$dp = (g\,\rho_o\, e^{c\,p} - 4Y/\Delta D)\,dz \qquad (8)$$

where:
c = compressibility
p_0 = top pressure amplitude
ρ_o = top cement density
Integrating (8) gives pressure at depth as follows:

$$\int_0^p (dp/e^{c\,\Delta p}) = (g\,\rho_o\, e^{c\,\Delta p} - 4Y/D) \int_{zo}^{z} dz \qquad (9)$$

or

$$e^{c\,\Delta p} - 1 = -c\,(g\,\rho_o - 4Y/D)\,(z - z_0) \qquad (10)$$

or

$$p(z) = p_0 - (1/c)\,\ln[1 - c\,m\,(z - z_0)] \qquad (11)$$

where:
z_o = depth at the top of section of interest; and

$$m = g\,\rho_o - 4Y/\Delta D \qquad (12)$$

Equation 11 describes pressure at depth for a slurry having uniform value of structural strength throughout the annulus. If the compressibility of the well-slurry system is small, eq. 7 can be simplified using Taylor series expansion around a point (p, ρ) as: $\rho = \rho_o\,(1 + c\,\Delta p)$. The pressure formula becomes:

$$p(z) = p_0 + (1/c)\,\{\exp[c\,m\,(z - z_0)] - 1\} \qquad (13)$$

For small compressibility, eqs. 11 and 13 give almost identical results. It can be proven that when a pressure pulse (p_0) is applied to slurry characterized by static gel strength (G) and yield point (Y) there exists a critical depth (Z) of slurry structure breakdown for each value of p_0. The slurry yields at the yield point above the critical depth while static gel strength controls structural breakdown below the critical depth. Critical depth may be calculated as follows:

$$Z = (p_0 - Y)\Delta D / 4Y \qquad (14)$$

Bottomhole pressure gradients in annulus above and below depth Z are different due to different structural strengths of cement in these two sections. Pressure at any depth can be calculated from eqs. 11 or 13 by using the following substitutions:
For $z < Z$:

$z_0 = 0$; and, Y = Yield Point (Y)

and, for $z >= Z$:

$z_0 = Z$; and, Y = Gel Strength (G)

5.1.1 Application of Static Model

Using the mathematical model, one can predict a change in bottomhole pressures and design an appropriate amplitude of the pressure pulse. The concept of bottomhole pressure control is shown in Fig. 18. Clearly, a relatively small pressure pulse may restore bottomhole pressure that has been lost due to gelation. The restored pressure is maintained even after the load is removed. Therefore, this method may use small pressures and avoid fracturing the hole.

Also, with this mathematical model the pressure pulse amplitude may be related to the entire pressure change in the well's annulus. Therefore, proper design of TCP should consider an increase of pressure above the initial slurry gradient during the TCP treatment. However, most

of the increased pressure section will be contained in the upper casing. Moreover, the amplitude of TCP pulse can be designed such that the previous casing shoe will not be fractured.

Another design parameter is the required value of the bottomhole pressure overbalance, which is not necessarily the pressure at the end of slurry placement. Therefore, an optimum amplitude of pressure pulse can be determined for a specific set of borehole conditions, as shown in Fig.18.

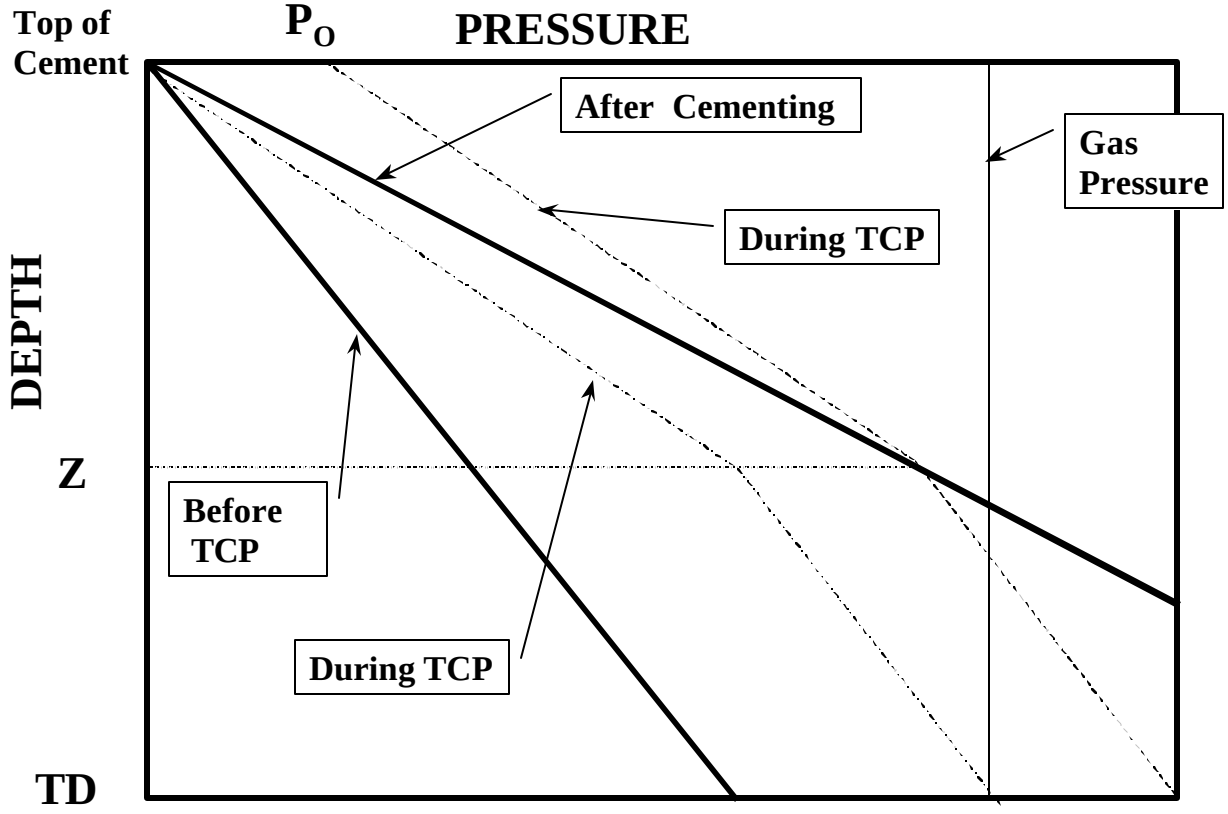

Figure 18. Conceptual change of pressure in cement column resulting from pressure pulse, p_0

An example calculation of the TCP method is presented below using the following input data:

- 16-in conductor pipe at 1,000 ft;
- 10 $^3/_4$-in surface pipe at 4,045 ft;
- TCP pulse amplitude, p_0 = 300 psi;
- 13.8 #/gal cement slurry;

Cement slurry properties two hours after cementing are:

- static gel strength, G = 450 #/100 sq.ft.;
- yield point, Y = 150 #/100 sq.ft.; and
- system compressibility, $c = 125 \cdot 10^{-6}$ 1/psi.

The results are shown in Fig. 19. Comparison of the plots "Before pulsing" and "After pulsing" shows that the difference of the two pressures increases with increasing depth. Thus the mathematical model verifies results and observations made in the field experiments reported above in Figs. 8 and 9. Other results of the example calculations are summarized in Table 3.

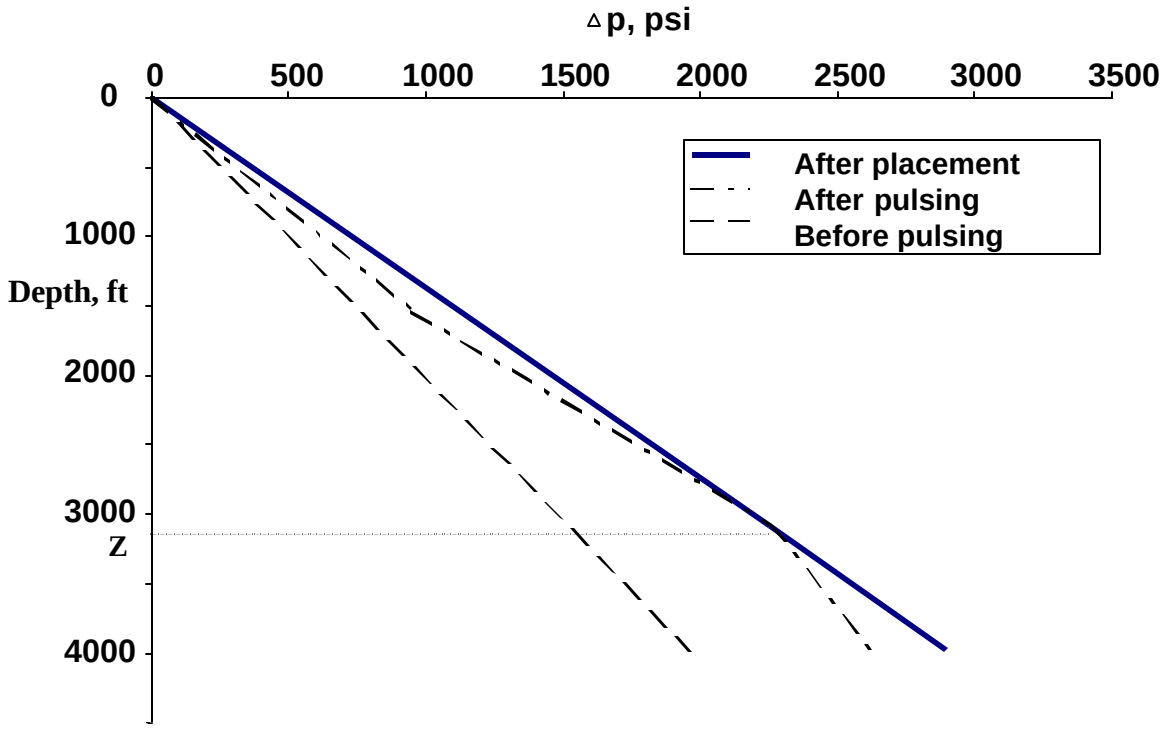

Figure 19. Predicted restoration of bottomhole pressure with cement pulsation

Table 3. Summary of example calculations (300 psi amplitude)

PARAMETER	UNIT	VALUE
Depth of TCP influence, Z	ft	3,150
Initial pressure @ Z	psi	2,260
Pressure @ Z during TCP	psi	2,548
Initial pressure @ TD	psi	2,903
Pressure @ TD before TCP	psi	1,961
Pressure @ TD during TCP	psi	2,942
Pressure @ TD after TCP	psi	2,641
Initial pressure gradient	psi/ft	0.75
Maximum pressure gradient due TCP	psi/ft	0.81
Depth of maximum pressure gradient	ft	3,150

In summary, the static model includes basic phenomena of the process and provides insight regarding the process design that can be explained as follows:

- Scientific evidence supports the concept of periodic and intermittent breakdown of a cement structure during its dormant period. Therefore, duration of resting periods (between pressure pulses) becomes a design variable to be determined.

- A simple analytical model developed in this research relates the pressure pulse amplitude to the entire distribution of pressure in the cement column during and after the treatment. The model reveals that the bottom part of the cement column may remain unaffected by the treatment. Also, the model provides an analytical tool for designing the desired pressure amplitudes that should be increased with time.

This research provides a theoretical proof of the behavior observed in the field experiments - an amplification of the top pressure pulse with depth. Moreover, the analytical model suggests that the amplifying effect will diminish below a critical depth.

5.2 Wave Propagation Model

For a number of reasons, a mathematical model of pressure wave propagation was deemed necessary in this work. These can be summarized as:

- Knowledge of displacement amplitude change with depth: This information is necessary for determination of the depth at which pulsation does not lead to slurry liquification;
- Need for the evaluation of the annular compressibility and its effect on pressure pulse propagation: The annular compressibility includes compressibility of cement slurry and rock in the open hole section. Compressibility controls slurry motion that is critical in this technology.
- Need for the prediction of the top cement displacement change in time: Seeing how pressure pulse needs to be adjusted to meet design objectives is important;
- Need for the evaluation of adverse effects that TCP might have on borehole stability.

The mathematical model was based on a momentum equation for the borehole annulus filled with Bingham plastic fluid. The reason for using the Bingham plastic rheological model was its simplicity together with reasonable accuracy for cement slurries. (The Herschel-Bulkley model may be slightly more accurate but it leads to non-linear equations, which are much more difficult to solve.) Other rheological models without yield point appeared to be inadequate. The Bingham plastic model by itself is not a time-dependent model. Both plastic viscosity and yield point, however, can be expressed as functions of time, thus adding time dependence to the model.

The following assumptions were made in the derivation and solution of the momentum equation:

- Cement moves as a plug;
- There is a sharp interface between cement and displacing fluid (gas or water);
- Effects of gas or water diluted, trapped or mixed with cement as a result of pulsation are ignored;
- Cement density is constant.

The momentum equation combined with the material balance equation for Bingham plastic fluid is:

$$\frac{\partial^2 y}{\partial t^2} - s^2 \cdot \frac{\partial^2 y}{\partial z^2} + \frac{12 \cdot m_p}{r \cdot (r_2 - r_1)^2} \cdot \frac{\partial y}{\partial t} + \frac{3 \cdot t_y}{r \cdot (r_2 - r_1)} - g = 0 \qquad (15)$$

Solution of this equation is in complex space. The real portion of the solution (Manowski and Wojtanowicz, 1998) is:

$$y = y_o \cdot e^{-b z} \cdot \cos(a \cdot z - w \cdot t) + \frac{1}{2} \cdot \frac{z^2}{s^2} \cdot \left(\frac{3 \cdot t_y}{r \cdot (r_2 - r_1)} - g \right) \qquad (16)$$

where:

$$a = \sqrt{\frac{w}{s^2}\cdot\sqrt{\left(\frac{12\cdot m_p}{r\cdot\left(r_2-r_1\right)^2}\right)^2+w^2}\cdot\cos\left(\frac{f}{2}\right)} \tag{16-1}$$

$$b = \sqrt{\frac{w}{s^2}\cdot\sqrt{\left(\frac{12\cdot m_p}{r\cdot\left(r_2-r_1\right)^2}\right)^2+w^2}\cdot\sin\left(\frac{f}{2}\right)} \tag{16-2}$$

$$f = \arctan\left(\frac{12\cdot m_p}{r\cdot w\cdot\left(r_2-r_1\right)^2}\right) \tag{16-3}$$

where:

E = modulus of elasticity	c = compressibility	g = acceleration of gravity
p, P = pressure	r = radius	s = acoustic wave velocity
t = time	T = wave period	$\bar{v}$ = average velocity
y = displacement amplitude	z, Z = depth	α = parameter
β = parameter	$\dot{g}$ = shear rate	ϕ = parameter
μ = viscosity	ν = Poisson's ratio	ρ = density
τ = shear stress	ω = angular frequency	

and the subscripts are:

1 - inner	2 - outer	C - casing
r – rock	b - bottom	c - cement
o - initial	p - plastic	y - yield (point)
w - wall		

Upon examination of the first component of eq. 16, we notice that for the depth z=0 and for time increasing from 0 to the half period of one pulsation cycle (5-10 sec), the value of cosine function will decrease from 1 to 0. This makes downward displacement negative and upward displacement positive, as measured from the initial position. Also, eq. 16 describes displacement *y* of cement particles whose initial position is *z*. Moreover, the equation is invalid when the wave is reflected from the bottom.

Equation (16) describes displacement of particles as a function of time and depth due to the application of forced oscillatory motion at the top. However, for analysis of CP we are more interested in the displacement amplitude. After re-grouping of terms, eq. (16) yields (Manowski, 1997):

$$y_{amp} = y_o\cdot e^{-\beta z} - \frac{1}{2}\cdot\frac{z^2}{s^2}\cdot\frac{3\cdot\tau_y}{\rho\cdot\left(r_2-r_1\right)} + \frac{1}{2}\cdot\frac{z^2}{s^2}\cdot g \tag{17}$$

Equation (17) describes the displacement amplitude as a function of depth, pulse frequency, acoustic wave velocity and cement properties. The first term on the right side of the equation sign represents the contribution of plastic viscosity and wave frequency to the attenuation of the pulse; the second term represents the contribution of the yield point to the attenuation and finally the last term comes from the weight of the fluid and it acts so as to increase the amplitude rather than attenuate it.

5.2.1 Downhole Pressure Prediction

The ability of the theoretical model to predict downhole pressure is important for the design and verification of TCP as it may offer an insight into the treatment depth and performance. Pressure can be measured more conveniently and accurately than displacement. Thus, monitoring pressure changes during the application of TCP is a way of assessing the efficiency of TCP.

Pressure at any depth can be combined with displacement *y* using the following formula (Binder, 1997):

$$\frac{\partial p}{\partial z} = -\rho_o \cdot s^2 \cdot \frac{\partial^2 y}{\partial z^2} \tag{18}$$

Combining eq. 16 with eq. 18 and performing suitable differentiation results in:

$$\frac{\partial p}{\partial z} = \rho_o \cdot y_o \cdot e^{-b \cdot z} \cdot w \cdot \sqrt{\left[\frac{12 \cdot m_p}{\rho \cdot (r_2 - r_1)^2}\right]^2 + w^2} \cdot$$
$$\cdot \left[\cos(\alpha \cdot z - w \cdot t) \cdot \cos\varphi - \sin(\alpha \cdot z - w \cdot t) \cdot \sin\varphi\right] -$$
$$- \rho_o \cdot \frac{3 \cdot t_y}{\rho \cdot (r_2 - r_1)} + \rho_o \cdot g \tag{19}$$

Pressure at any depth can then be computed by integrating equation 19 from the top of the cement (z=0) to a given depth z=Z:

$$P = \rho_o \cdot y_o \cdot s^2 \cdot \{\cos\varphi \cdot [e^{-b \cdot Z} \cdot \{\alpha \cdot \sin(\alpha \cdot Z - w \cdot t) - b \cdot \cos(\alpha \cdot Z - w \cdot t)\} + \alpha \cdot \sin(w \cdot t) + b \cdot \cos(w \cdot t)]$$
$$+ \sin\varphi \cdot [e^{-bZ} \cdot \{b \cdot \sin(\alpha \cdot Z - w \cdot t) + \alpha \cdot \cos(\alpha \cdot Z - w \cdot t)\}$$
$$+ \alpha \cdot \cos(w \cdot t) + b \cdot \sin(w \cdot t)]\} - \rho_o \cdot \frac{3 \cdot t_y}{\rho \cdot (r_2 - r_1)} \cdot Z + \rho_o \cdot g \cdot Z \tag{20}$$

5.3 Wave Propagation Study and TCP Design Concept

An investigation of the influence of cement rheology on propagation of pressure pulse was performed in a series of parametric studies. In all cases, the amplitude of displacement was computed using eq. 17. Table 4 presents data used in the first study.

Three isolated effects are discussed here. First, the contribution of plastic viscosity to attenuation of the wave will be presented. This is achieved by neglecting the yield point and fluid density terms in eq. 16, that simplifies equation (16) as:

$$y_{amp} = y_o \cdot e^{-\beta z} \tag{17-A}$$

Table 4. Initial data for parametric study

Amplitude:	12	ft
Plastic viscosity	70	cp
Density	16.2	#/gal
Outer diameter	14.75	in
Inner diameter	10.75	in
Yield point	690	lbf/100 sq ft
Wave velocity	3,000	ft/s
Wellbore depth	16,000	ft

Next, the contribution of yield point is taken into account through the following relationship:

$$y_{amp} = y_o - \frac{1}{2} \cdot \frac{z^2}{s^2} \cdot \frac{3 \cdot \tau_y}{\rho \cdot (r_2 - r_1)} \qquad \text{(17-B)}$$

Finally the individual effect of fluid density is taken into account by comparing displacement amplitude computed from eq. 16 with and without the last term, i.e.:

$$y_{amp} = y_o \cdot e^{-\beta z} - \frac{1}{2} \cdot \frac{z^2}{s^2} \cdot \frac{3 \cdot \tau_y}{\rho \cdot (r_2 - r_1)} \qquad \text{(17-C)}$$

The plots in Fig. 20 show individual effects of plastic viscosity and yield point on the distribution of displacement amplitude with depth computed from eqs. 17A and 17B, respectively. The third plot in Fig. 20 is the actual amplitude computed from eq. 17 with all effects included. Note that the effect of plastic viscosity appears to be small over the whole length of the borehole, while the effect of yield point increases with depth (it is proportional to the depth squared).

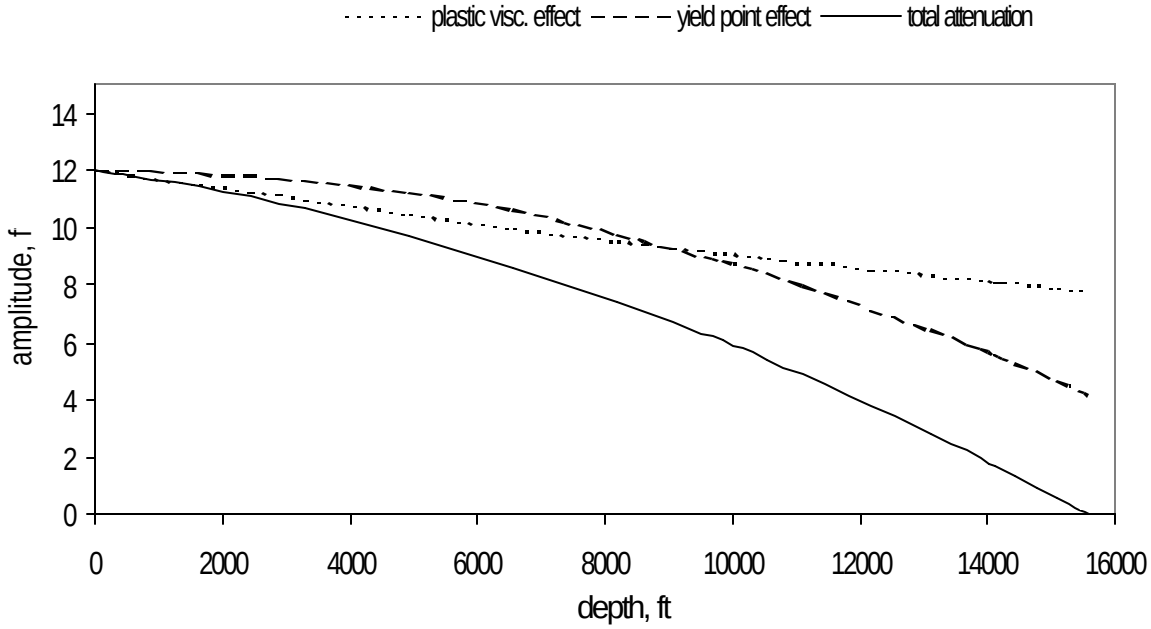

Figure 20. Individual effects of plastic viscosity and yield point on TCP pressure wave attenuation in cement column

The effects of annular size and fluid density are shown in Figs. 21 and 22 by comparing the difference between results from eq. 17C (all effects except for density) with those from eq. 17 (all effects). Plots in Fig. 21 pertain to a 14.75”/10.75” casing/casing annulus, while those in Fig. 22 - a 12.25”/9.625” casing/casing annulus. Table 5 gives the input data for Fig. 22. Obviously, the cross-sectional area of this annulus is much smaller than that in Fig. 21.

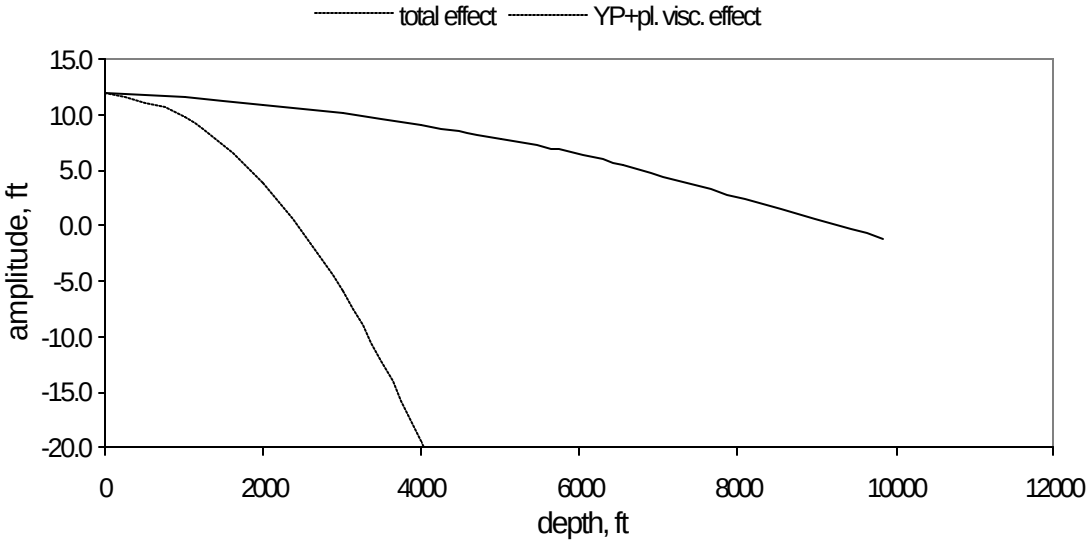

Figure 21. Effect of fluid density on pressure pulse attenuation, parametric study 14.75”/10.75” casing/casing annulus

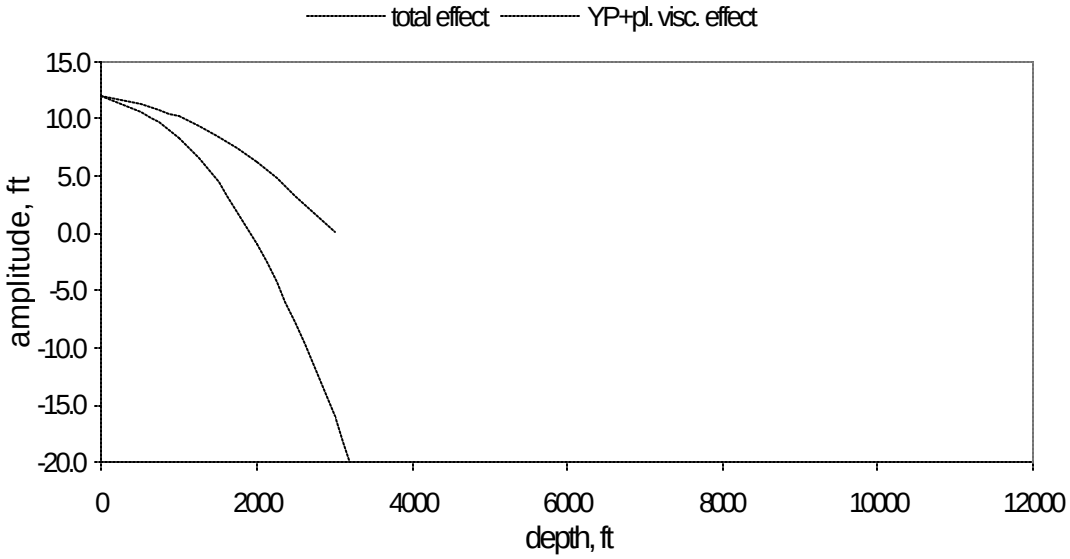

Figure 22. Effect of weight of fluid on pressure pulse attenuation, parametric study 12.25”/9.625” casing/casing.

Comparing Fig. 21 and Fig. 22, shows that in the case of a smaller annulus, pressure wave is attenuated much stronger. This is mostly due to the fluid weight effect: there is much more fluid present in the 14.75 in./10.75 in. annulus, and the weight is helping the fluid break the gel, thus the wave propagates much deeper. In conclusion, we can say that the most disadvantageous conditions for wave propagation is the combination of high - yield point cement slurry in a small annulus.

Table 5. Initial data for a parametric study

amplitude:	12	ft
plastic viscosity	70	cp
Density	16.2	#/gal
outer diameter	12.25	in
inner diameter	9.625	in
yield point	690	lbf/100 sq ft
wave velocity	3,000	ft/s
wellbore depth	16,000	ft

5.3.1 Top Cement Displacement Change During TCP - Model vs. Field Data

Using the wave propagation model, eq. 16, and experimental data on cement rheology and compressibility, one can calculate the attenuation of displacement amplitude with depth if the top displacement amplitude is known. A field procedure for monitoring top displacement has previously been developed (Haberman and Wolhart, 1997) using either water or gas pulse generators. Fig. 23 presents data from top displacement monitoring. Two patterns of top displacement are shown. One pattern gives almost constant displacement with respect to time over the monitoring period. According to eq. 17, this would mean that cement liquidity is maintained over that period. The other curve shows a constant decline of the amplitude of displacement. Apparently, the TCP treatment was unsuccessful here. Such behavior was explained by the rapid dehydration of the cement slurry, which occurred due to the lack of filtrate cake on the wall of the well (the well was drilled with brine) combined with the lack of fluid loss additive in the slurry (Haberman and Wolhart, 1997).

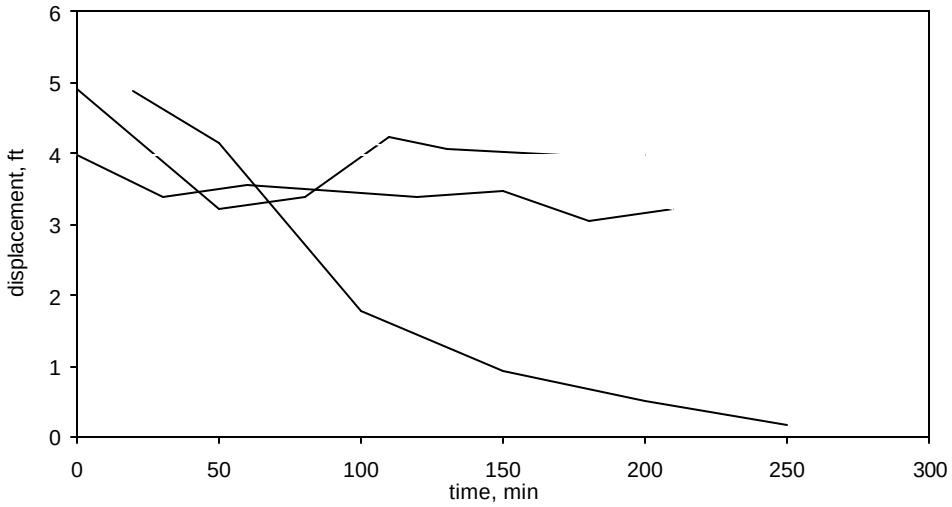

Figure 23. Cement top amplitude logs from three shallow wells in Permian Basin during TCP (Haberman and Wolhart, 1997)

According to the mathematical model discussed above, there are two possible mechanisms of top displacement reduction in time: system compressibility decrease or reduction of the pulsed cement volume (Haberman and Wolhart, 1997). System compressibility is defined here as cement compressibility and borehole expansion. Since, according to the results of experiments, cement compressibility does not change much and the rock mechanical properties are constant, compressibility of the annular system can be assumed constant. Thus, the same top

pressure pulses should generate the same displacements over long periods of time. Some plots in Fig. 23 confirm this theory.

The other explanation implies that as the bottom portion of cement starts to set, cement transforms from liquid state to solid state thus eliminating volumetric compressibility altogether. In the result, only the upper liquid section of cement slurry is compressed which results in reduction of the top displacement. The problem with this theory is the delay required for slurry to set. Since slurry setting takes several hours to occur there should not be any early reduction of top cement displacement shown in Fig. 23. (That's why the authors explained this pattern by water loss mechanism.) The shortcoming of the "compressibility" theory is that it disregards another phenomenon at work - pressure transmission attenuation caused by the slurry rheology change.

Thickening of cement slurry results in the increase of yield point and plastic viscosity that, in turn, reduces the displacement amplitude throughout the cement column, as modeled by equation 17. Ads the thickening process may not be uniform at all depths, the pattern of top cement displacement may also differ. Thus, monitoring of the top cement displacement during the TCP treatments may provide important information on cement seal quality.

5.4 Conceptual Design of CP Treatment Schedule

The objective is to design TCP operation so as to selectively minimize transition time of cement and thus minimize the likelihood of gas or water intrusion into the cemented column. At the same time, hydrostatic pressure exerted by the reciprocated cement column must exceed water or gas zone pore pressure. Thus, there are two design criteria for this method: selective minimization of cement transition time and bottomhole pressure maintenance. The theoretical basis for this method is derived for the rapid hydration period of cement. This period is specific for a slurry at given pressure and temperature conditions.

5.4.1 Selective Control of Cement Transition Time

This technique can be used to minimize the transition time of cement slurry for a given minimum volume of cement in the wellbore at a given time. For this technique to be feasible, both estimates of time at which tail cement starts to set at the bottom and at which the lead cement starts to thicken at the top are needed. These estimates can be obtained from cement consistometer test as time to reach 70 units of consistency. This time, commonly referred to as cement “thickening time,” is routinely evaluated in service companies’ laboratories. Then the rate of cement thickening in the well computed as the ratio of the depth of the well divided by the difference between these two times can be computed. Beginning from the time when cement starts to set at the bottom, the pressure pulse applied at the top is decreased in such a way that the depth to which this pressure wave can reach will decrease precisely at the rate equal to the cement setting rate computed earlier. All the cement that is below that depth is allowed to set, while all the cement above is being reciprocated, thus it exerts high hydrostatic pressure. The assumption is made that at a certain time, the pressure wave is allowed to reach top of the rectangle marked V_1 (see Fig. 24).

Volume V_1 is left undisturbed and sets freely at the time T_1. If there is a gas or water zone opposite the volume V_1, it will not be allowed to flow into the setting cement during the transition time of volume V_1 because of the high hydrostatic pressure. By the time the subsequent volumes V_2 and V_3 advance into the transition phase and hinder the transmission of hydrostatic pressure, volume V_1 will have already developed enough mechanical resistance to seal the zone hydraulically.

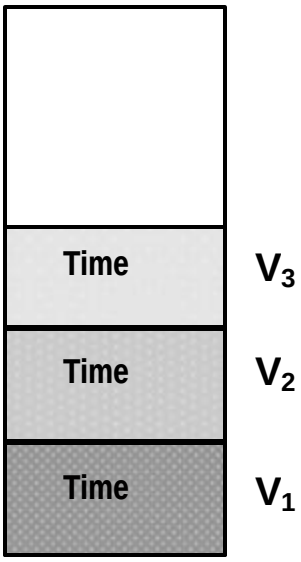

Figure 24. Selective minimization of cement slurry transition time, T ($T_1<T_2<T_3$)

It is therefore important that this cement volume that is no longer being reciprocated sets quickly. The only way this requirement can be ensured is to stop reciprocation during the accelerated hydration period after the dormant period. The aforementioned API thickening time test should give us an estimate of this critical time. It is important to stress here that cement reciprocation cannot proceed into the accelerated hydration period because of the set cement compressive strength decline occurring when cement is sheared for too long in that period, (Hartog et al., 1983). Reciprocation must be ceased during the shaded period shown in Fig. 25.

5.4.2 Maintenance of Bottomhole Pressure Overbalance

The first criterion, while minimizing transition time, does not guarantee that pressure exerted by cement column will not decrease below the pore pressure of a porous formation at any time. There is a need, thus, to monitor hydrostatic pressure in the cement column.

For this criterion to be practically achievable, an estimated depth of the offending zone with its pore pressure should be known. If at any time hydrostatic pressure exerted by the cement column next to that zone comes near the pore pressure in the zone, then pressure pulse strength cannot be decreased further, as per the first criterion, but it needs to be maintained or even increased so that the zone is not allowed to flow into the annulus.

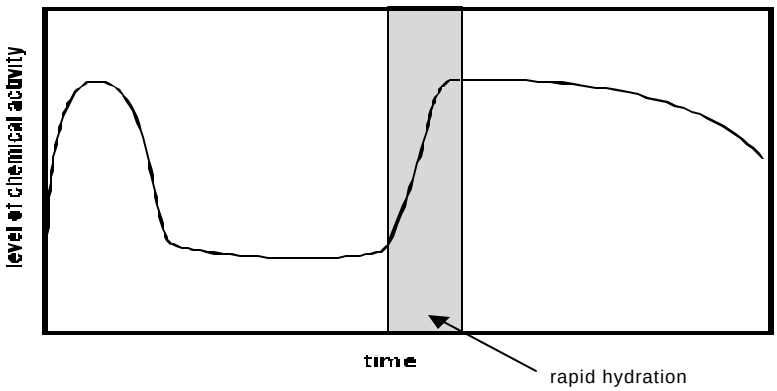

Figure 25. Level of chemical activity in cement as evidenced by temperature changes

These conditions must be maintained long enough to enable the cement next to the formation to set and seal the annulus. The time necessary for cement to set and seal the annulus

will depend on specific conditions, such as the type of cement used, depth and temperature of the well, etc.

Finally, it should be pointed out that there are some cement systems that do not exhibit rapid hydration as shown in Fig. 25. Additives used in these systems (not necessarily retarders) slow down the hydration process (i.e., development of strength after the dormant period).Also, there are cement systems that give hydration more rapid than that for neat cement. Thus, care will have to be exercised with each cement system designed to work with TCP.

6. FULL-SCALE EXPERIMENTAL STUDY OF CEMENT PULSATION WITH CEMENT-LIKE SLURRY

The general objectives of this full-scale experimental study were to validate the underlying concepts for cement pulsation and the factors influencing its effectiveness. The experiments were designed specifically to address the following issues:

1. How do fluid properties and well geometry influence the transmission of hydrostatic pressure in a fluid column?
2. Is pulsation any more effective than applying the same pressure as a single step increase?
3. How do factors, such as fluid properties, well geometry, and pulse characteristics, influence the effectiveness of pressure pulsation in restoring pressure transmission through a column of thixotropic fluids?

6.1 Selection of Cement-like Slurry

Cement could not be used in the LSU wells for the full-scale experiment due to the obvious reason that the cement setting would permanently plug the wells. Therefore it was necessary to formulate cement-like slurries to conduct repetitive full-scale experiments. Formulation of the cement-like slurry was based on the thixotropic and gelation properties of cement slurries. The cement-like slurry was developed to give properties similar to those of cement during early gelation.

6.1.1 Equipment and Testing Procedures

The rheological and other properties of the cement and cement-like slurries were characterized using the following equipment.

6.1.1.1 Fann Coaxial Cylinder Viscometer

Six rotational speed (600, 300, 200, 100, 6, 3 rpm) Fann 35 coaxial viscometers were used to characterize the rheological properties of the cement and cement-like slurries. In this viscometer, the outer sleeve rotates with a constant speed around a stationary bob. Standard sleeve and bob size were used (Sleeve ID = 1.45 in. and Bob OD = 1.358 in.). The slurry contained in a cup is sheared between the outer sleeve and the inner bob. In our experiments, the cement and cement-like slurries were sheared for one minute at 300 and 600 rpm respectively before any readings were taken.

6.1.1.2 Atmospheric Consistometer

This was used to precondition the cement slurries before static gel strength and rheological measurements were taken. The Atmospheric consistometer has a preset rotational speed of 150 rpm. The cement slurry prepared per API Specification 10B was poured into the consistometer cup and conditioned in the atmospheric consistometer for about 20 minutes at a set temperature.

The consistency of the cement and cement-like slurries were also measured with the atmospheric consistometer.

6.1.1.3 MACS Analyzer

The MACS Analyzer was used to measure the Thickening Time and Static Gel Strength (SGS) of the cement slurries at high temperatures and pressures. The cement slurry was prepared according to API Specification 10B and poured into the slurry chamber of the MACS Analyzer. The cement and cement-like slurries were preconditioned for 15 and 10 minutes respectively at a rotational speed of 100 rpm before static gel strength measurements were taken. A rotational speed of 0.5 degree per minute was used to measure the SGS.

6.1.1.4 Static Gel Strength Analyzer (SGSA) Model 4270

The SGSA was used to measure the SGS and compressive strength of the cement slurries at high temperatures and pressures. The cement slurries were prepared per API specification 10B and then preconditioned in the Atmospheric Consistometer for 20 minutes before pouring into the SGSA for testing. The current design of this apparatus precludes its use for measuring SGS with fluids that do not develop compressive strength. Therefore, it was only used to measure cement properties.

6.1.2 Thixotropic and Gelation Properties of Typical Cements

Two cement slurries, 15.6 ppg Class A and 16.4 ppg Class H cements were prepared as per API Spec. 10B for use in determining physical characteristics of typical cement slurries, see Table 6. Based on the results and studies of Class A and H cements, cement-like fluids were formulated using the concept of developing fluids with gel strengths that increase progressively with time to a high value of 50 – 100 lbs/100 sq ft and then essentially stop building gel strength, see Tables 7 and 7-A and Figures 26 and 26-A. Several formulations were experimented with, including Maraseal, Permseal (both recommended by Benchmark) and different combinations of bentonite and polymer either hydroxyethylcellulose (HEC) or polyanionic cellulose (PAC), see Table 8 and Fig. 27.

Table 6. Properties of Class A and Class H cements

Cement Type	Class A	Class H
Density,ppg	15.6	16.4
10 sec. Gel Strength, lbs/100 sq ft	24	16
10 min. Gel Strength, lbs/100 sq ft	35	22
Plastic viscosity, cp	90	65
Yield point, lbs/100 sq ft	72	51
Thickening Time @ 110° F and atmospheric pressure (100 Bc), mins	238	345
Water Loss @ 100 psi and 78° F, cc/ 30 min	117	138
Free Water, cc	2	6.2
Compressive Strength with 4% $CaCl_2$ added to slurry and measured at 3000 psi and 140° F UCA Initial Set: 50 psi, (Hrs)	1:20	1:28
UCA Strength: 500 psi, (Hrs)	1:51	1:49

Table 7. Gel strength of cement and cement-like fluids

		Viscometer Readings (Gel Strength, lbf/100 sq. ft.)							
	Time,	Cement Type		8% Bentonite		Other Fluids		8% Bentonite Plus	
TIME	(mins)	Class A	Class H	Freshwater	pH water	Maraseal	Organic	0.25% PAC	0.5% PAC
10 secs	0.17	24	16	9	15	1	2	26	33
10 mins	10	35	22	22	32	1	2	56	64
30 mins	30	56	45	35	42	1	3	70	78
1 hr	60	210	99	38	45	2	3	74	86
2 hrs	120	>300	>300	39	46	2	3	76	92
4 hrs	240			43	50	2	3	82	95

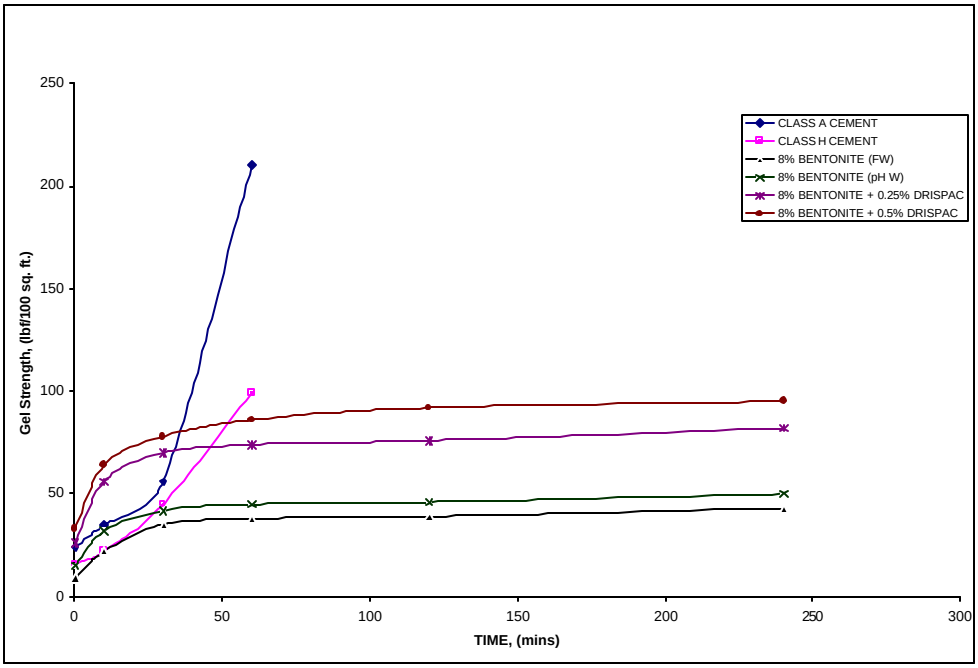

Figure 26. Gel strength versus time of cement and cement-like fluids

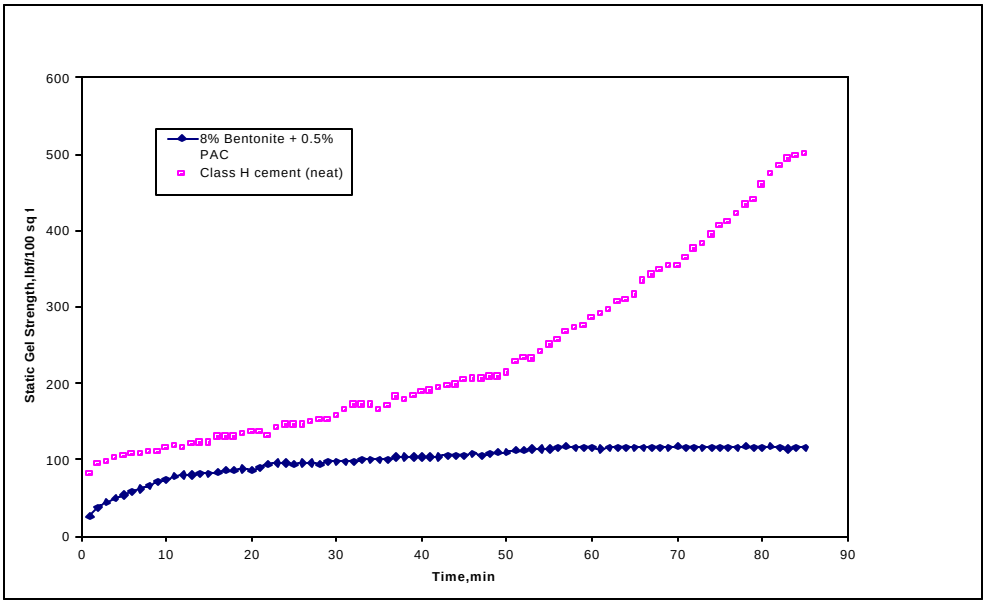

Figure 26-A. Static gel strength versus time of cement and cement-like slurry measured with the MACS analyzer

Table 7-A. Static gel strength of Class H cement and the cement-like slurry measured with the MACS analyzer

Time, min	SGS lbf/100 sq ft	
	Cement-like slurry	Class H cement(neat)
1	26	82
2	38	94
3	44	98
4	50	102
5	54	106
6	58	108
7	62	108
8	66	110
9	72	110
10	74	116
11	78	118
12	80	116
13	80	120
14	82	122
15	82	122
16	84	130
17	86	130
18	86	130
19	88	134
20	86	136
21	90	136
22	94	132
23	96	142
24	96	146
25	94	146
26	96	146
27	96	150
28	94	152
29	98	152
30	98	158
31	98	166
32	98	172
33	100	172
34	100	172
35	100	166
36	100	170
37	104	182
38	104	178
39	104	184
40	104	188
41	104	190
42	104	194
43	106	196

Time, min	SGS lbf/100 sq ft	
	Cement-like slurry	Class H cement(neat)
44	106	198
45	106	204
46	108	206
47	106	206
48	108	208
49	110	208
50	110	214
51	112	228
52	112	234
53	114	232
54	114	242
55	114	250
56	116	256
57	118	268
58	116	272
59	116	276
60	116	286
61	114	290
62	116	296
63	116	306
64	116	310
65	116	316
66	116	334
67	116	342
68	116	348
69	116	354
70	118	354
71	116	364
72	116	376
73	116	382
74	116	394
75	116	406
76	116	412
77	116	422
78	118	434
79	116	440
80	116	460
81	118	474
82	116	484
83	114	494
84	116	498
85	116	500

Table 8. Consistency of cement and cement-like fluids

						8% Bentonite plus					
Class A cement		Class H cement		8%Bentonite		0.25% PAC		0.50% PAC		0.10% HEC	
Time,(mins)	C.U (Bc)	Time,(mins)	C.U (Bc)	Time,(mins)	C.U (Bc)	Time,(mins)	C.U (Bc)	Time,(mins)	C.U (Bc)	Time,(mins)	C.U (Bc)
0	12	0	9	0	9	0	7	0	11	0	15
40	16	20	10	10	9	10	8	12	11	10	21
130	18	45	11	20	9	40	9	30	11	20	22
170	35	60	12	30	9	55	9	50	11	30	22
192	48	80	12	40	9	70	9	75	11	40	22
210	65	100	13	50	9	90	9	165	11	50	22
230	88	122	14	60	9	120	9	225	11	60	22
234	94	133	15	70	9	155	9	305	11	65	23
236	96	180	22	80	9	245	9	365	11	95	24
237	98	193	25	90	9	280	9			125	23
238	100	218	32	100	9	340	9			155	23
		240	36	120	9					185	23
		253	45	150	9					215	23
		296	63	180	9					245	23
		320	75	210	9					275	23
		328	80	240	9					305	23
		335	85								
		342	90								
		345	100								

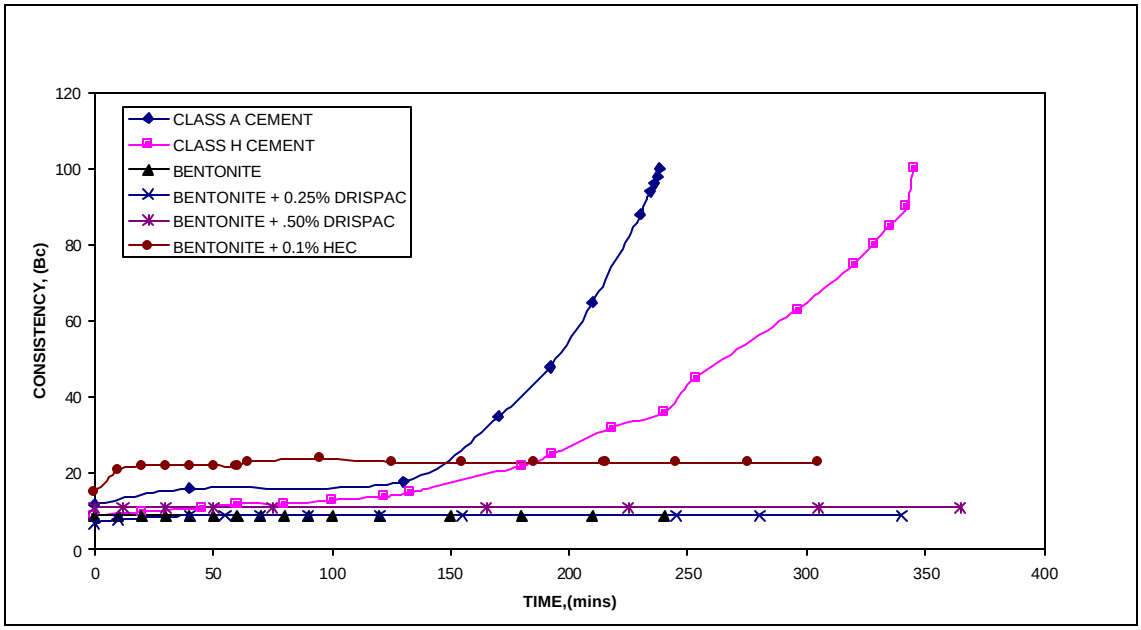

Figure 27. Consistency versus time of cement and cement-like fluids

We determined the maximum gel strength that could theoretically be displaced from the LSU well number one, see Fig. 28, for the proposed CP experiment. Given the well geometry, pump parameters and an appropriate safety factor at the LSU Well facility, a maximum gel strength in the range of 50 – 100 lbs/100 sq ft was calculated using eq. 21 (Bourgoyne et al, 1991).

$$\Delta P = \frac{t_g}{300(D_2 - D_1)}\Delta L \quad \text{.....(21)}$$

where:

ΔP – pressure differential required to break circulation, psi,
τ_g – static gel strength, lbs/100 sq. ft.,
D_2 – internal diameter of outer pipe, in.,
D_1 – external diameter of inner pipe, in.,
ΔL – depth, ft.

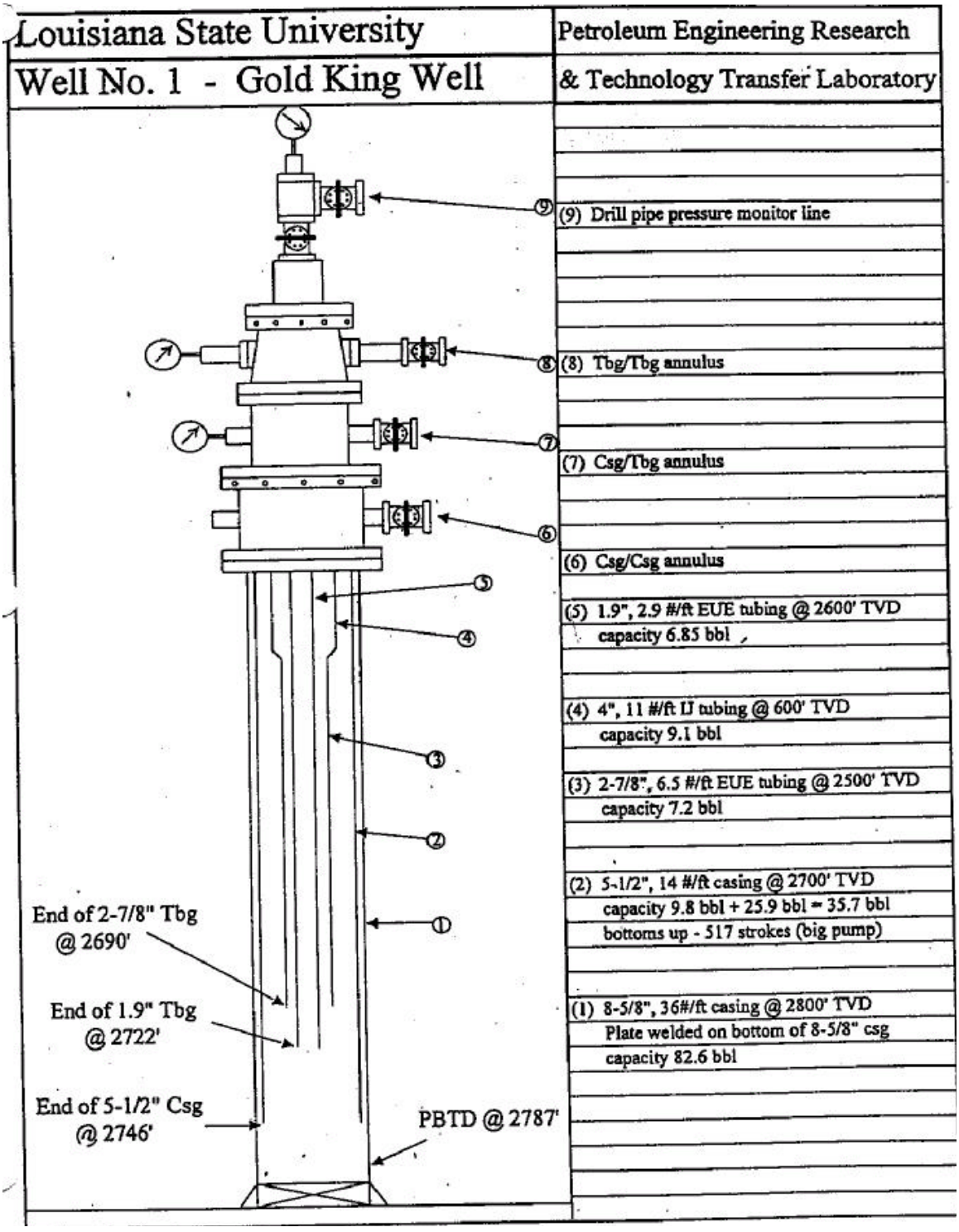

Figure 28. Wellbore sketch for LSU well #1

See Table 9 for a summary of the well geometry, gel strength and pressure to break circulation. Based on the thixotropic and gelation behavior of cement slurries in conjunction with our calculation for maximum gel strength that can be broken in the LSU well, we selected a candidate fluid that was 8% bentonite plus 0.5% PAC, see Table 10. This formulation gave an initial gel strength of 25 lbs/100sq ft and 10 minute gel strength of 55 lbs/100sq ft. See Table 11 for rheological properties of this formulation.

Table 9. Summary of pressure to break circulation in well #1

Well Name:	LSU #1
Depth:	2722.00
Tubing	
I.D.	1.61
Gel Str	100.00
Diff Press	563.56
Annulus 1	"tapered"
O.D.	2.44
I.D.	1.90
Gel Str	100.00
Diff Press	1677.14
Annulus 2	"tapered"
O.D.	5.01
I.D.	4.00
Gel Str	100.00
Diff Press	896.57
Annulus 3	
O.D.	7.83
I.D.	5.50
Gel Str	100.00
Diff Press	390.25

Table 10. Formulation of candidate fluid

Component	Quantity per bbl.	Quantity for Well #1
Water,(bbls)	0.96	121.42
Bentonite, (lbs).	29.2	3693.26
Caustic soda, (lbs)	0.11	13.3
PAC, (lbs)	0.15	18.47
Aldacide-G, (lbs)	0.4	50.57
Total volume of slurry,(bbls)	1	126.43

Table 11. Properties of candidate fluid

Density,pp	8.8
10 sec. Gel lbs/100 sq	25
10 min. Gel lbs/100 sq	55
Plastic viscosity,	27
Yield point, lbs/100	30
Yield stress, lbs/100	12

6.2 Test Description

6.2.1 Experimental Design

The overall objective of cement pulsation is to maintain pressure transmission through a fluid that builds gel strength when static. Therefore these experiments needed to measure pressures in the test well that are equivalent to downhole pressures in a cemented annulus. The experiment was conducted in LSU well #1, which is 2800 ft deep, having a 8-5/8 in. casing cemented at 2800 ft. One 5-1/2 in. casing and two tubing strings (1.9 in. and 2-7/8 in. tapered) are suspended from the well head inside the 8-5/8 in. casing, see Fig. 28. These provide three annuli extending from the surface to various depths, all below 2690 ft. The total of four flow paths from surface to TD provided both the sections to be filled with cement-like slurry and a means for sensing pressures and pressure changes within the overall length of slurry.

The tubing and the 8-5/8 in. x 5-1/2 in. outer annulus were completely filled with the cement-like slurry. The 8-5/8 in. x 5-1/2 in. outer annulus simulated a common geometry for production casing cement jobs. The tubing simulated a narrower, smaller capacity section, extending from the 8-5/8 in. x 5-1/2 in. to the bottom of the hole. Because this section actually terminates at the surface, a pressure equivalent to the pressure at the bottom of the cemented annulus can be measured at the wellhead. The two intermediate annuli were completely filled with water. The pressure on these annuli was recorded and represents the pressure halfway down a cemented annulus, which in our case was also the location of the geometry change.

A detailed experimental design and procedure to conduct this experiment was prepared and is included as Appendix 8. The actual experimental procedure evolved as the test progressed and is described in detail in the following subsections.

6.2.2 Preparation of Cement-like Slurry at the Well Facility

Cells 1 and 2 of tank #1 were filled with 100 bbls of fresh water and 37 sacks (100 lbs/sack) of bentonite were mixed in the water and left to prehydrate for about 60 hours. Cell 3 of tank #1 was filled with 21.4 bbls of fresh water and 13.3 lbs of caustic soda was added and stirred until completely dissolved. The high pH water in cell 3 was mixed with the slurry in cells 1 and 2 for about 2 hours. Then, 18.47 lbs PAC-L were added slowly while stirring. Finally an hour later, 5.5 gallons of Aldacide-G, a biocide, was added and thoroughly mixed. The density and the rheological properties were measured and found to be lower than expected. The slurry was left static for about 14 hours after which it was agitated for about 2 hours and the density and rheological properties were measured and still found to be low. Three sacks of bentonite were added to the slurry and stirred for about 2 hours. The density and rheological properties were measured. The actual properties of this fluid before and after placement in the well are given in Table 23.

Table 23. Properties of cement-like slurry before and after placement in well #1
(T = dial reading)

Sample before pumping into well #1											
TIME	Time,(min.)	T_{600}	T_{300}	T_{200}	T_{100}	T_6	T_3	GS	PV	YP	YS
10sec.	0.17	79	54	43	30	12	12	20	25	29	12
10min	10	82	56	45	32	12	12	55	26	30	12
30min.	30	87	59	47	33	13	13	67	28	31	13
Sample after pumping into well #1											
TIME	Time,(min.)	T_{600}	T_{300}	T_{200}	T_{100}	T_6	T_3	GS	PV	YP	YS
10sec.	0.17	84	57	45	32	12	12	20	27	30	12
10min	10	87	60	47	33	14	14	57	27	33	14
30min.	30	89	60	48	34	14	13	68	29	31	12
1hr	60	95	64	51	35	13	12.5	80	31	33	12
16hrs	960	98	67	53	37	13	12.5	125	31	36	12

6.2.3 Placement of Cement-like Slurry in LSU Well #1

Well #1 was circulated with water for about 10 minutes. The lines were tested against the Swaco choke at 3500 psi for 5 minutes. The cement-like slurry described in Tables 22 and 23, was circulated down through 8-5/8 in. x 5-½ in. annulus and up the 1.9 inch tubing until the annulus and the tubing were completely filled with the slurry. The two smaller annuli were both left full of fresh water and are referred to subsequently as the intermediate annuli or water leg. All valves on the X-mas tree were closed and the well was left static for 16 hours to let the slurry build up gel strength inside the well. The recorded pressures on the strings after 16 hours static were 150 psi on the outer annulus, 105 psi on the intermediate annulus and 10 psi on the tubing. The estimated pressure differential at the surface between the slurry filled columns and the water leg due to density difference between the slurry and water was 56 psi.

6.2.4 Overview of Test Sequence

Four kinds of tests were conducted to identify and assess the factors influencing loss of pressure transmission and effectiveness of cement pulsation. The initial tests measured pressure response to a constant rate of increase in applied pressure. This style test was repeated to evaluate gelation effects. Pulsation tests, including different amplitudes and periods were conducted with the CTES pulsation unit. Tests with a constant pressure applied to the annulus were performed for comparison to pulsation. Finally, tests with simulated pulsation, using a pump were conducted to assess the effects of smaller pulses and longer periods.

6.3 Results of Tests to Determine Pressure Required to Establish Pressure Communication Through a Gelled Fluid

In order to quantify the actual pressure required to establish pressure communication in the outer annulus, we pressurized the outer annulus slowly to enable us observe any pressure response on the intermediate annuli. The gel strength of the slurry in the well after 16 hours static was approximately 125 lbs/100 sq ft, see Table 23. Using eq. 21 and this gel strength value gave a predicted pressure differential required to break the gel in the outer annulus to be about 488 psi, see Table 24. The point at which a response is observed in the intermediate annuli, indicates the initial pressure communication, which conceptually means the gel in the outer annulus is being broken.

Table 24. Estimated pressure differential to re-establish communication

Time	Gel Strength lbs/100 sq ft	Yield Stress lbs/100 sq ft	Pressure differential based on gel strength (psi)		Pressure differential based on yield stress (psi)	
			Casing	Tubing	Casing	Tubing
10 mins.	55	12	215	310	47	68
2 hours	92	12	359	518	47	68
20 hours	125	12	488	704	47	68
67 hours	130	12	507	732	47	68

Test 1: The 8-5/8 in. x 5-½ in. annulus was pressurized in 10 psi increments, and the pressure observed and recorded for all four string pressure gauges. Initially there was no change in pressure gauge readings on tubing and intermediate annuli. At a 50 psi increase in pressure above base pressure in the 8-5/8 in. x 5-½ in. annulus, the intermediate annulus pressure increased from 85 psi to 100 psi indicating the break of gel in the 8-5/8 in. x 5-½ in. annulus, while the tubing gauge did not record any change in the pressure, see Fig. 29.

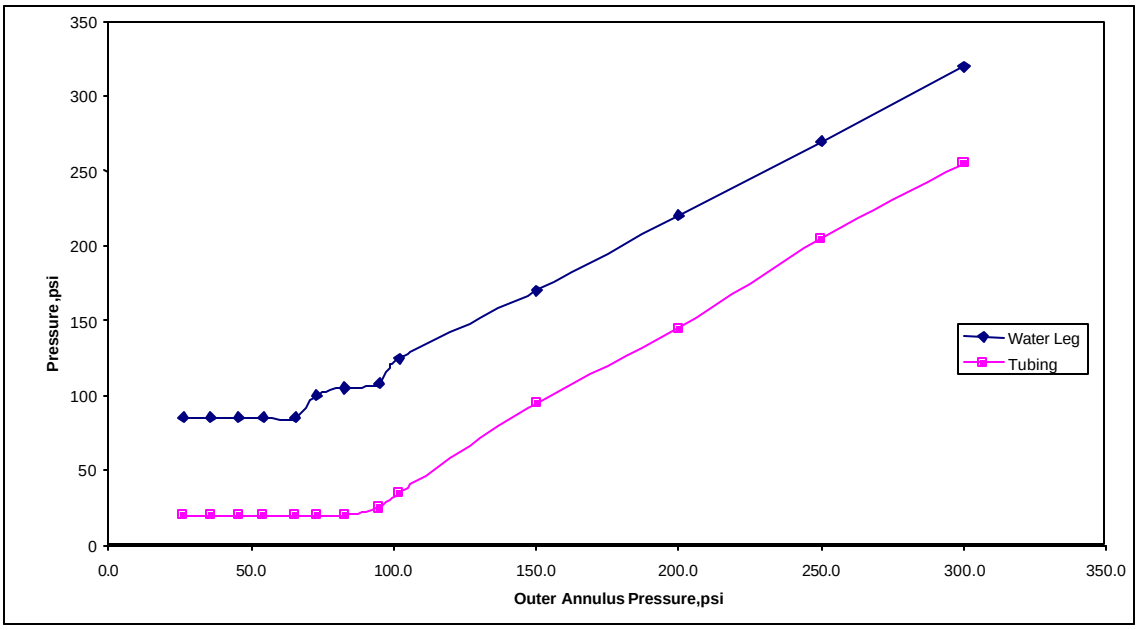

Figure 29. Test 1- Pressure transmission test performed on outer annulus

On continued pressurizing of the 8-5/8 in. x 5-½ in. annulus, the tubing pressure also started increasing when the 8-5/8 in. x 5-½ in. annulus pressure increased by 70 psi above the base pressure, while the intermediate annulus pressure kept on increasing. The differential pressures required to initiate pressure communication between strings were much less than estimated based on gel strength. The annulus was pressurized up to 300 psi and corresponding readings of all pressure gauges were recorded, see Appendix 1. The final pressure differential across the tubing and the 8-5/8 in. x 5-1/2 in. annulus were 9 and 36 psi respectively. The pressure differential on the tubing was lower than expected and than observed in most subsequent tests. Consequently, we currently view it as an unexplained anomaly.

Test 2: In preparation to perform an equivalent test with declining pressures, about 40 psi pressure was bled off from the intermediate annulus, and the pressure readings on all the gauges were recorded. All pressure gauges showed decrease in pressure indicating pressure communication between tubing and all annuli. However, the response on the outer annulus was much larger (62 psi change) than on the tubing (5 – 10 psi change), probably because there was a greater pressure differential trapped on the outer annulus to begin with. The well was left static for about an hour to allow build up of gel strength and was then bled through 5-1/2 x 4 in. annulus again in 10 psi decrements and the corresponding water volume bled off was measured. Initially, the outer annulus pressure gauge showed a slight decrease in pressure while the tubing head pressure was fairly constant at about 215 psi. The final pressure differential across the tubing and the 8-5/8 in. x 5-1/2 in. annulus were 61 and 36 psi respectively. Again, much less pressure was required to initiate pressure communication than that expected based on eq. 21. Although the test was terminated before the pressure differentials had peaked, communication with both the outer annulus and the tubing had been initiated. The pressure to initiate communication on the outer annulus was far less than either 312 psi (based on 1 hour gel strength) or 488 psi (based on 20 hour gel strength) as predicted by eq. 21 and the measured gel strength.

6.4 Results of Pulsation Tests with CTES Unit

The CTES pulsation unit was used in the pulsation test on well #1. The specifications of this equipment are as follows:

Size: 9' L x 6'W x 8'H
Weight: 5,300 lbs
2 Tanks (ASME): 200-gallon capacity and 200 psi operating pressure.

It has sensors to monitor water level (volume), water tank pressure, air tank pressure and water supply flow. See attached photos in Appendix 9.

Prior to pulsation, the well was left static for 16 hours with no pressure on the outer (8-5/8 x 5-½ in.) annulus. The intermediate annulus (5-½ x 4 in.) pressure was bled off directly at the surface from 84 psi to 64 psi and the corresponding water volume measured was 1080 cc. No communication was observed on the tubing and outer annulus gauges.

Test 3: Pulsation on the 8-5/8 x 5-½ in. annulus was started with a 60 psi pulse. The pressure was raised to 60 psi and held for 20 seconds, depressurized and waited for 20 seconds (i.e. 20/20 seconds cycle), see Fig. 30-A. Before the next pulse was applied, the maximum pressures observed on all four gauges were recorded. For the first five pulses, the pressures remained the same, and then, the pressure in the intermediate annulus (5-½ x 4 in.) started increasing, while no pressure change was observed on the tubing pressure gauge, see Fig. 30. The same trend was observed up to 20 pulses with the pressure on the intermediate annulus increasing approximately 27 psi over its initial value in response to repeated pulsation. See Appendix 2 for detailed data. The pressures reported in Appendix 2 and subsequent discussions of pulsation tests are the maximum observed during pulsation. Comparisons between pulsation and simply applying a constant pressure are included in the section "Analysis of Results."

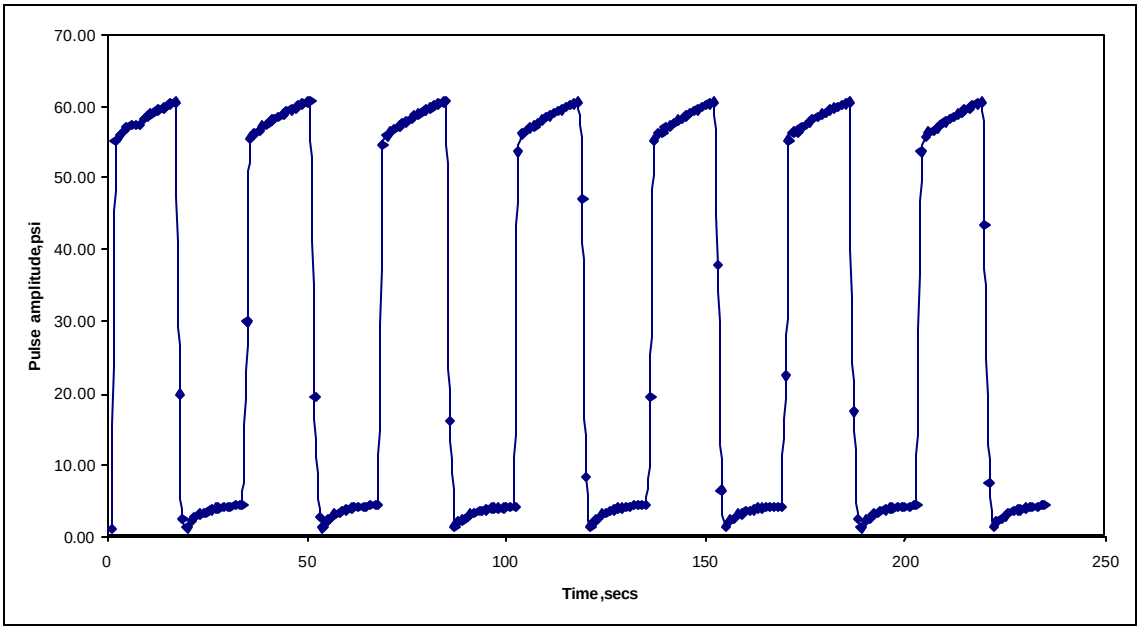

Figure 30-A. Pulsation during Test 3: 60 psi and 20/20 second pulsation cycle

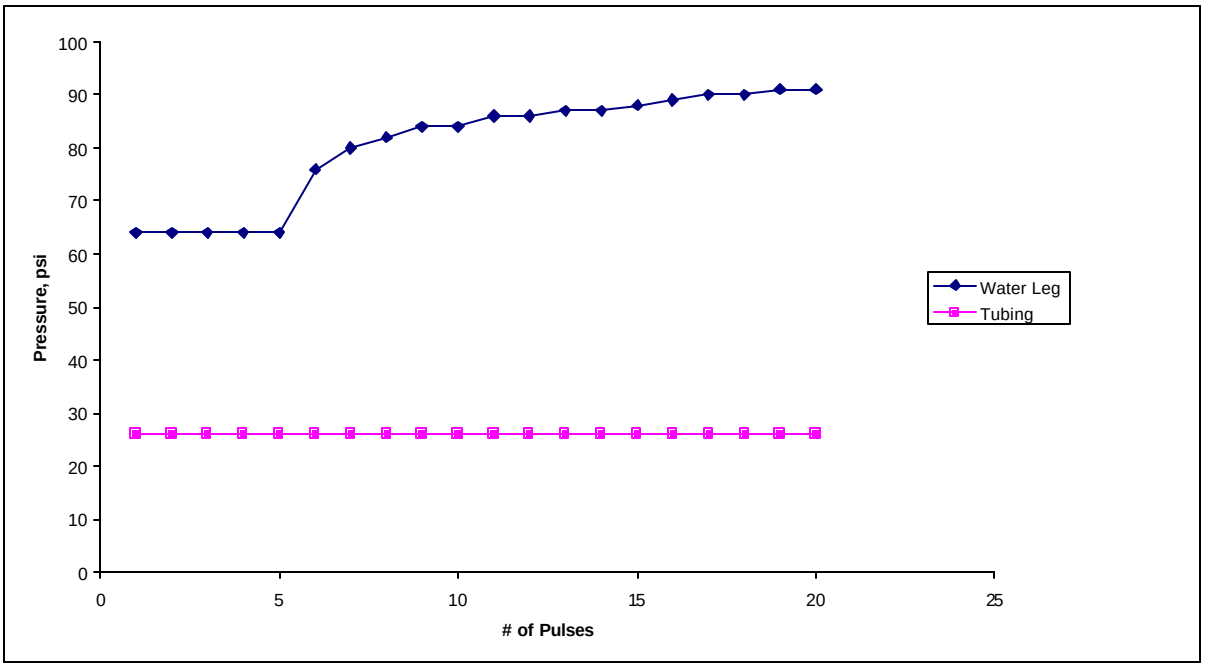

Figure 30. Test 3- Pressure response to pulsation with 60 psi pulse amplitude and 20/20 second cycle

Test 4: The pressure on the tubing side was then bled off from 26 psig to zero and the corresponding volume of slurry recovered was 1880 cc. This was intended to simulate the fluid and volume loss downhole after cement placement that can initiate flow after cementing. The pressure on the outer annulus remained constant at 4.2 psi, and the pressure on the intermediate annulus was constant at 86 psi. Then pulsation was continued with the same pulse magnitude and frequency as Test 3. The tubing pressure remained zero and there was a marginal change in the intermediate annulus (5-½ x 4 in.) resulting in peak pressures equal to those during Test 3, see Appendix 2.

Test 5: The pulse magnitude was increased to 66 psi with 20/20 second cycle. The pressure on the intermediate annulus (5-½ x 4 in.) increased gradually from 91 psi and stabilized at 100 psi after 20 pulses while the tubing pressure remained zero, see Fig. 31.

Test 6: The pulse magnitude was again increased to 85 psi with 20/20 second cycle. The pressure on the intermediate annulus (5-½ x 4 in.) increased gradually from 102 psi and stabilized at 117 psi after 10 pulses while the tubing pressure remained zero. The pulsation was continued with the same pulse magnitude and frequency. A slow increase in the tubing pressure began at this point. Both the tubing and the intermediate annulus pressures increased about 2 psi over the next 10 cycles and were still increasing slowly when pulsation was stopped.

Test 7: The pulse magnitude was maintained at 85 psi with 40/40-second cycle. The pressure on the intermediate annulus (5-½ x 4 in.) increased a few psi over the first 3 cycles and then remained constant at 124 psi, while the tubing pressure increased continuously with successive cycles from 3.7 psi to 18 psi indicating that the 40/40 second cycle was more effective than a 20/20 second cycle for this system.

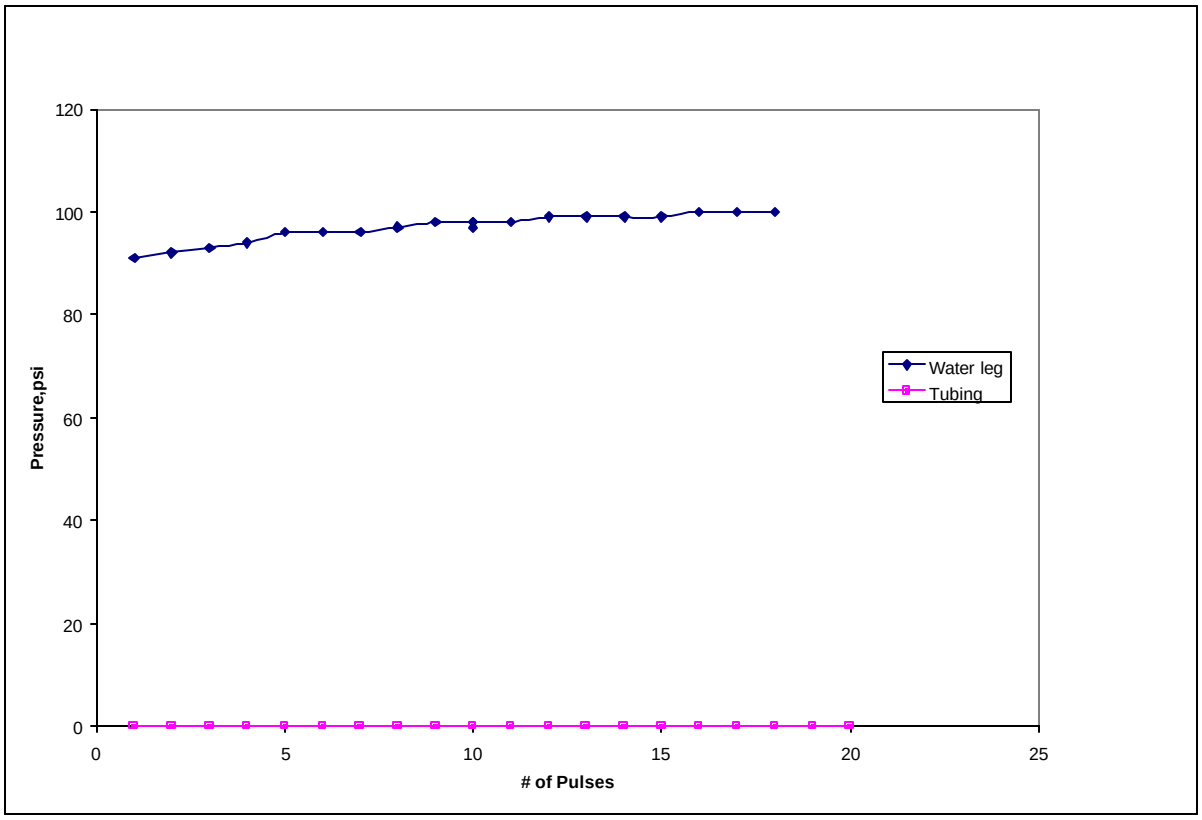

Figure 31. Test 5- Pressure response to pulsation with 66 psi pulse magnitude and 20/20 second cycle

Test 8: The pulse cycle was changed to 80/20 seconds. The tubing pressure increased more rapidly than with the 40/40 second cycle and stabilized at a pressure that was 25 psi higher than with the 40/40 second cycle, indicating that this cycle was even more effective. The intermediate annulus pressure (5-½ x 4 in.) increased slightly to about 128 psi and then remained almost constant. Both intermediate annulus pressure and the tubing pressure stabilized after 10 pulses with the intermediate annulus at 129 psi and tubing at 43.5 psi.

Test 9: The pulse cycle was then changed again to a 100/50 second cycle and no additional changes in the pressure gauge readings were observed. Consequently, it was deemed that increases in pulse duration beyond 80/20 seconds were unnecessary.

When the pulsation was stopped, the pressure on the intermediate (5-½ x 4) annulus dropped from 129 psi to 86 psi and the pressure on the outer annulus dropped to 4.7 psi. No change in the tubing pressure was observed indicating the fluid in the tubing was holding the changing differential pressure that resulted from stopping pulsation at the low pressure phase of the pressure cycle.

Test 10: A 110 psi and 80/40 second cycle pulse was applied to the outer annulus. The pressure on the intermediate annulus immediately increased from 86 psi to 150 psi and then stabilized at about 154 psi while the tubing pressure increased from 44.5 psi to 65.5 psi, see Figure 32. When the pulsation ended, the pressure on the intermediate annulus dropped to 84 psi. Then, 1560 cc of water was bled off from the intermediate annulus and the pressure dropped from 84 psi to 64 psi.

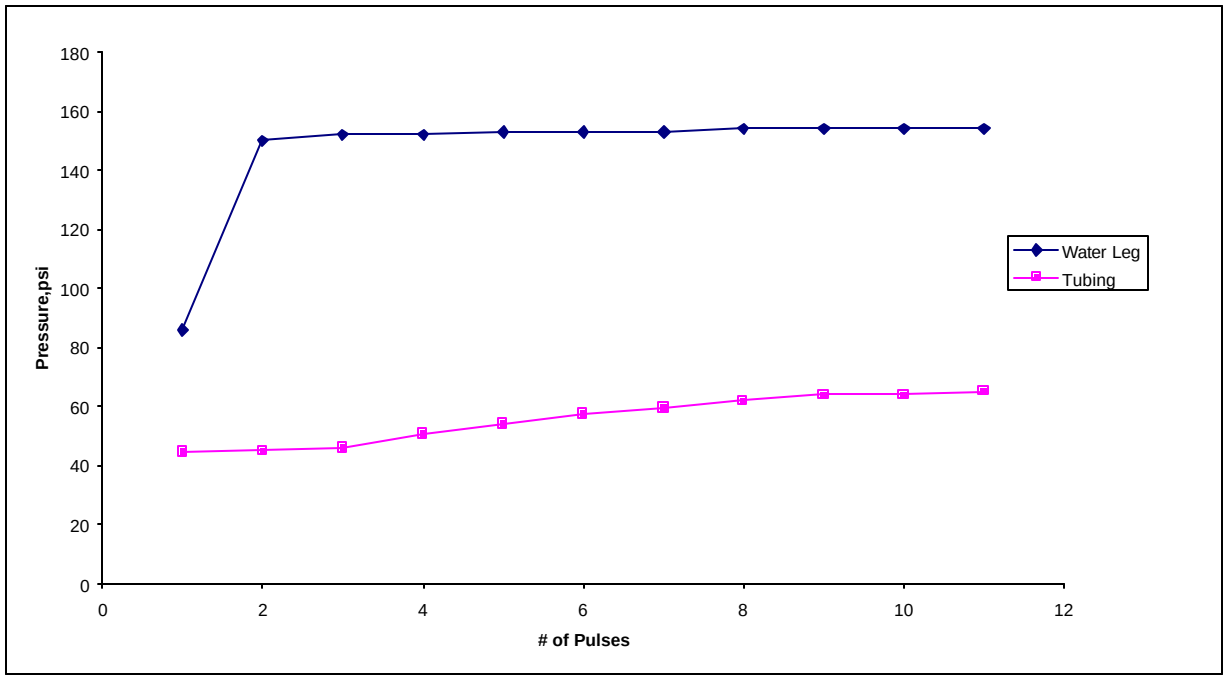

Figure 32. Test 10- Pressure response to pulsation with 110 psi pulse magnitude and 80/40 second cycle

Test 11: Before the start of this test, the tubing side pressure was bled off from 56 psi to zero to achieve an initial condition equivalent to a hydrostatic balance between all four fluid columns. The corresponding volume of slurry bled off was 2160 cc. A pulse of 110 psi and 60/40 second cycle was then applied. The intermediate annulus pressure increased to 146 psi immediately and eventually increased to 154 psi. The tubing pressure increased from 4 psi to 70 psi with successive pulses (total of 10 pulses). These results were almost identical to Test 10.

Test 12: For the final pulsation test, the pulse magnitude was increased to 130 psi with a 60/40-second cycle. The intermediate annulus pressure immediately increased to and then remained almost constant at about 180 psi, while the tubing head pressure increased from 75 psi to 91 psi with the application of five pulses, see Fig. 33.

Once the pulses were stopped, the tubing pressure dropped back from 91 psi to 78 psi and finally stabilized at 60 psi and the intermediate annulus pressure dropped from 181 psi to 94 psi and stabilized finally at 88 psi.

6.5 Results of Additional Pressure Transmission Tests

Following the pulsation tests, more tests were conducted to determine the effect of gel strength development over time and of pressure changing at different rates, for comparison with the pulsation tests. The general purpose was to investigate the impact of these factors on the loss of hydrostatic pressure transmission relating to gelation and the restoration of pressure transmission by application of additional pressure. A specific objective was to compare pulsation to the application of a constant pressure.

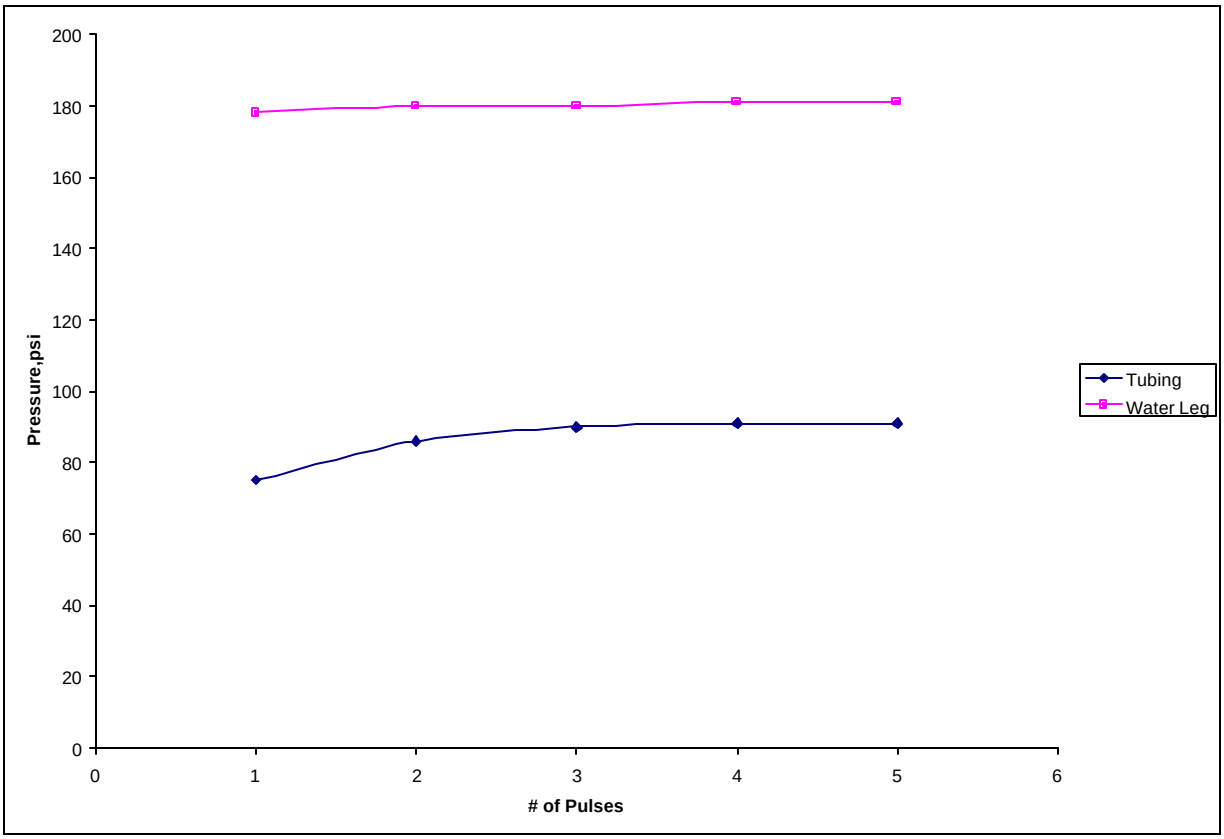

Figure 33. Test 12- Pressure response to pulsation with 130 psi pulse magnitude and 60/40 second cycle

Test 13: After leaving the well static for about 2 hours, we carried out the test described in Appendix 3 on the 1.9 in. tubing by increasing the pressure in 10 psi increments by pumping at a rate of about 1400 cc/min and recording the pressure on all the other gauges. When the tubing pressure reached the value of 90 psi, the intermediate annulus pressure started increasing. When the tubing pressure reached the value of 130 psi, the pressure on the 8-5/8 x 5½ in. annulus started rising. The tubing was ultimately pressurized to 200 psi and the other pressure readings of 200 psi on the intermediate annulus and 85 psi on the outer annulus were noted at stabilized conditions. Therefore the final differential pressures on the tubing and the outer annulus were 55 psi and 60 psi, respectively.

The pressure was then bled off from the tubing gradually to simulate fluid loss and/or volume shrinkage downhole and the corresponding pressure readings on the annuli were recorded. When the tubing pressure dropped to 69 psi, the intermediate annulus pressure started decreasing, see Appendix 3. Pressure communication with the outer annulus was not obvious, even after bleeding the tubing pressure to zero. This demonstrates that the cement-like slurry in the outer annulus was holding differential pressure, thus preventing bottom hole pressure maintenance. It also shows that the maximum pressure differential held by the fluid in the tubing was essentially the same, 52 psi, as in the first phase of this test, but in the opposite direction.

Test 14: After 20 hours of static conditions, another test was performed for comparison to both the previous test and to pulsation. The 8-5/8 in. x 5-1/2 in. annulus was pressurized continuously using the Haskel pneumatic pump to inject water and the pressures on the tubing and intermediate annulus were recorded after every 10 psi increment of pressure on the 8-5/8 in. x 5-

1/2 in. annulus. The test was continued until significant response was observed in both the tubing and intermediate annulus. The pump was stopped and waited a few minutes for the pressures to stabilize. The 8-5/8 in. x 5-1/2 in. annulus was then bled off gradually, and pressures on all strings were recorded for every 1000 cc of water bled off. The corresponding results are shown in Fig. 34 and Appendix 4.

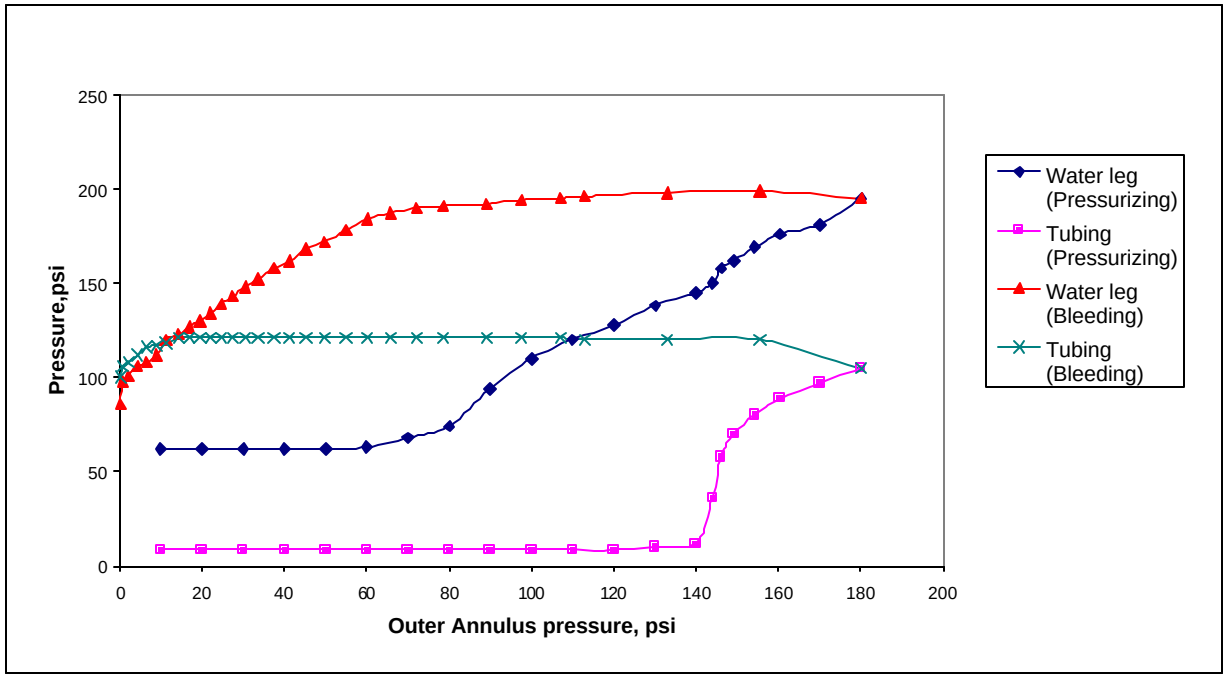

Figure 34. Test 14-Pressure transmission test after 20 hours static

Test 15; 16; 17; 18: This style test was repeated for static conditions of 42 hours, 2 hours, 10 minutes and 67 hours respectively. Similar trends of pressure response were observed for the different static times. See Figures 35, 36, 37, 38, and Appendix 5 for the corresponding results. The significance of these tests is that, the maximum pressure differential, see Figure 39-A, required to re-establish pressure communication in a fluid column increases with time as the gel strength increases, see Table 25 and Fig. 39. For example, the maximum pressure differential observed across the entire length of slurry when establishing pressure communication increased from 116 psi when the slurry was static for 10 minutes to 144 psi when the slurry was static for 67 hours. Conversely, the pressure differential of approximately 90 psi, across the entire length of slurry, opposing dynamic change does not change significantly for static times from 10 minutes to 67 hours.

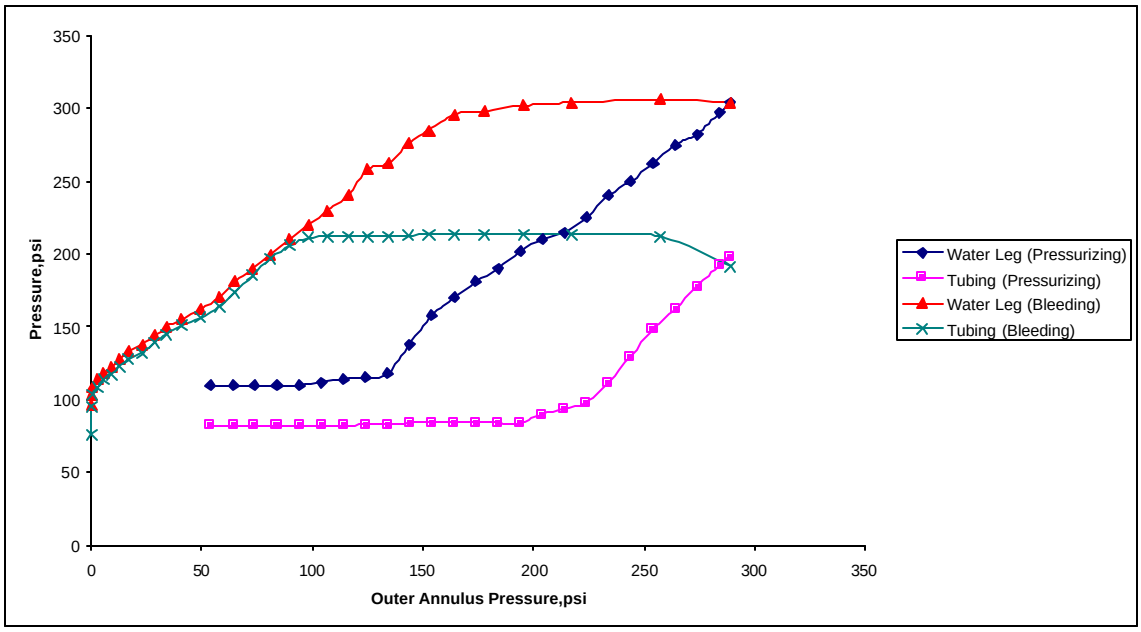

Figure 35. Test 15- Pressure transmission test after 42 hours static

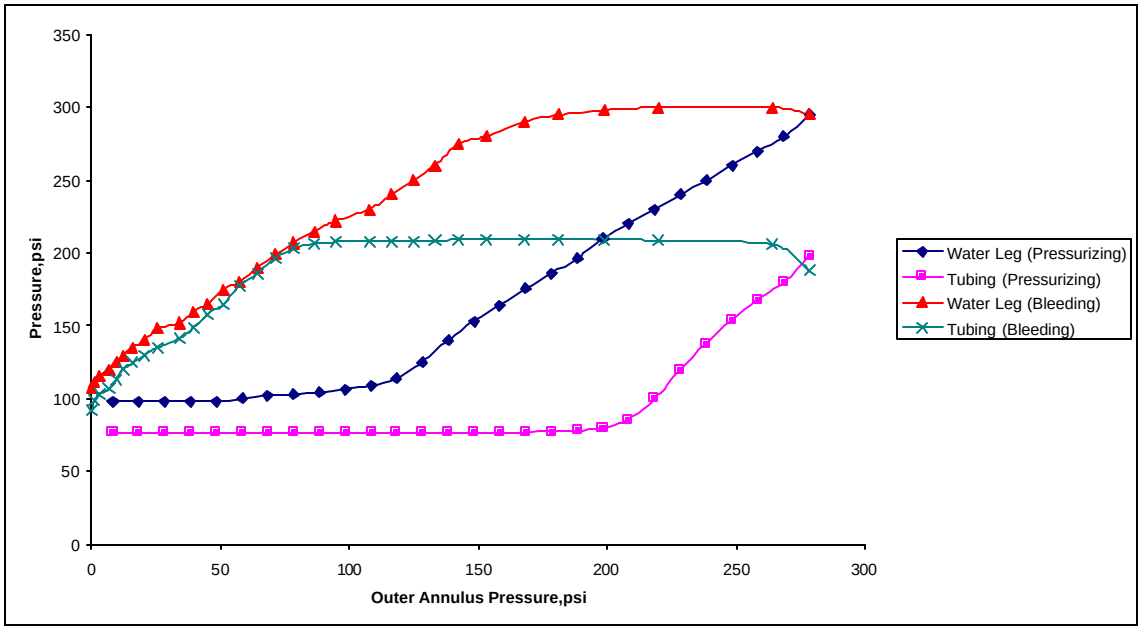

Figure 36. Test 16- Pressure transmission test after 2 hours static

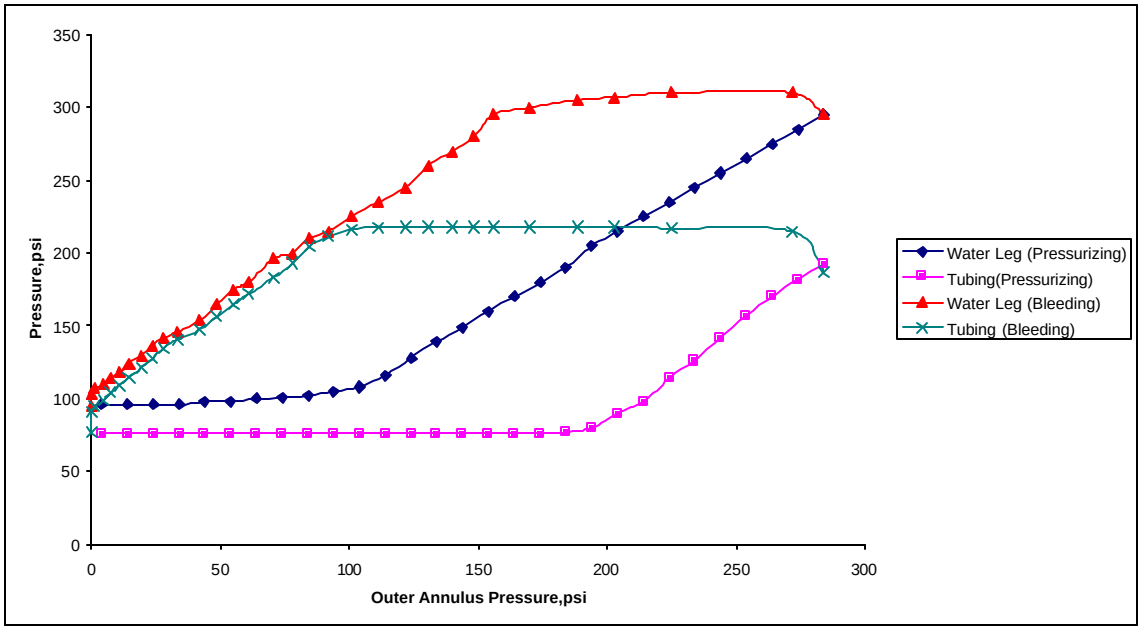

Figure 37. Test 17- Pressure transmission test after 10 minutes static

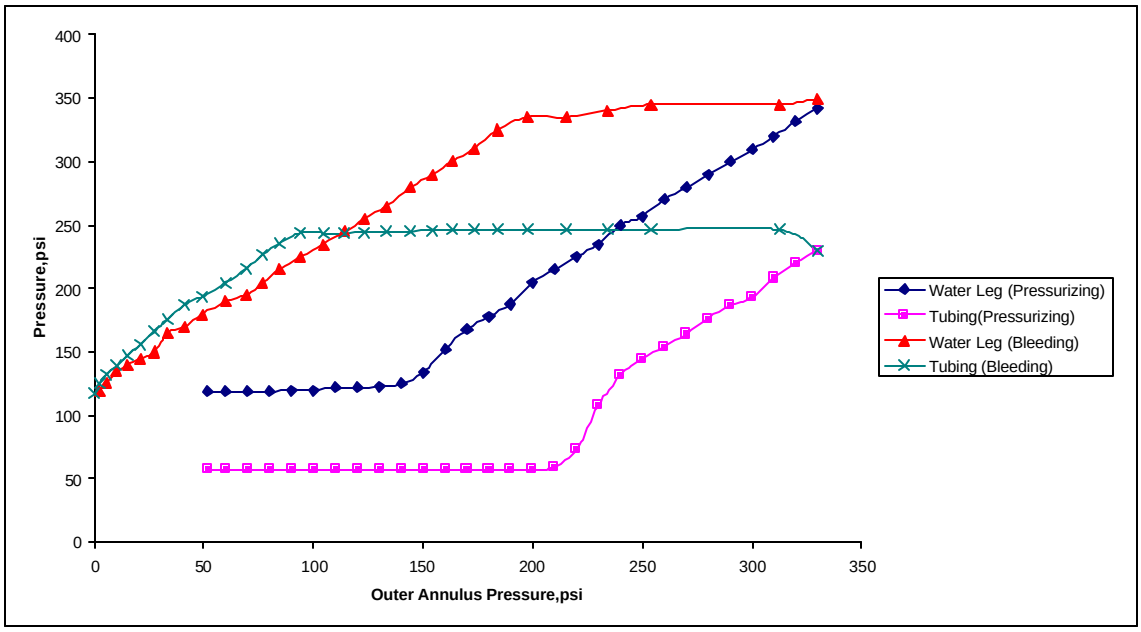

Figure 38. Test 18 - Pressure transmission test after 67 hours static

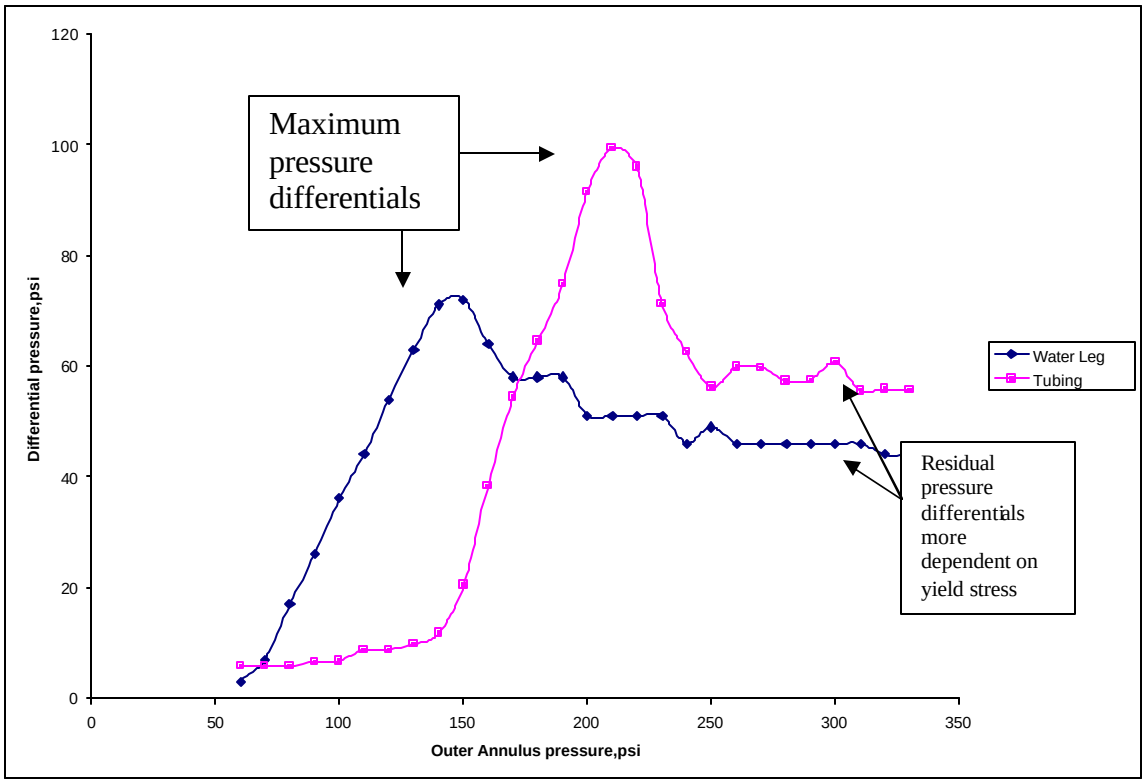

Figure 38-A. Pressure differentials during Test 18 after 67 hours

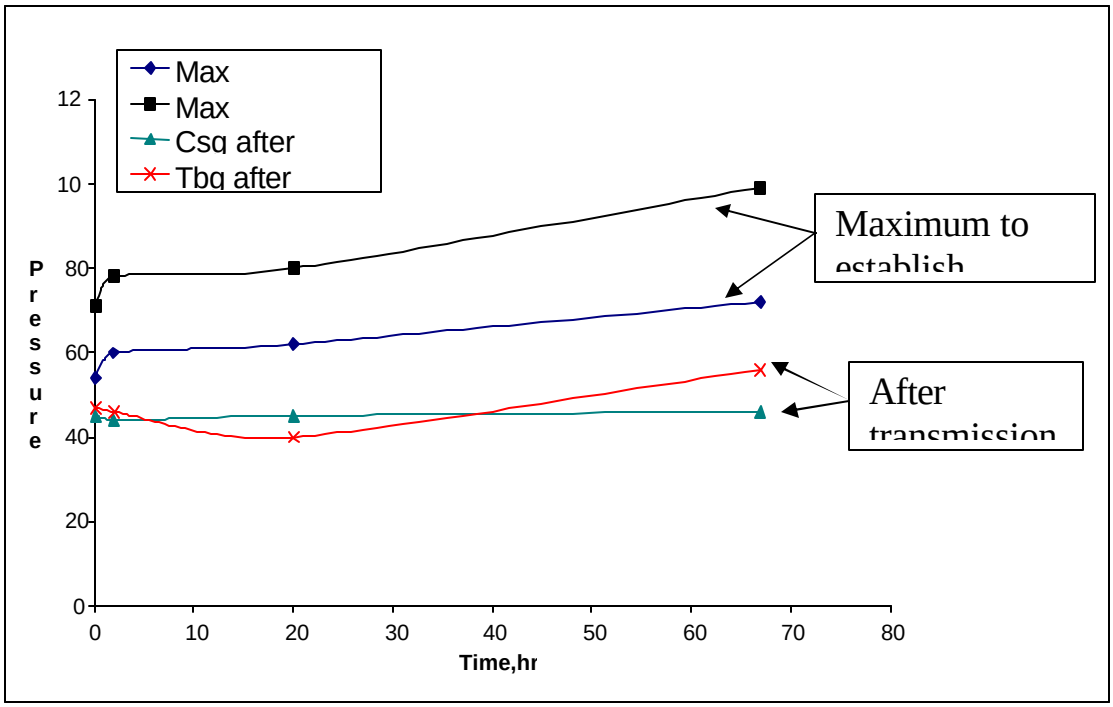

Figure 39. Pressure differential opposing pressure transmission for various static times

Table 25. Measured pressure differential to re-establish communication

Time	Gel Strength lbs/100 sq ft	Yield Stress lbs/100 sq ft	Initial pressure differential observed psi		Maximum pressure differential observed psi		Maximum pressure differential observed psi	Pressure differential after parallel trend psi	
			Casing	Tubing	Casing	Tubing	across csg/tbg	Casing	Tubing
10 mins	55	12	52	70	54	71	116	45	47
2 hours	92	12	55	74	60	78	122	44	46
20 hours	125	12	53	77	62	80	128	45	40
67 hours	130	12	71	93	72	99	144	46	56

To investigate the effect of a single stepwise pressure increase on pressure transmission without pulsation, we conducted several tests with a constant pressure on the outer annulus. These tests were intended to simulate the field practice of applying a constant pressure on top of the annulus after cementing it, for comparison to pulsation.

Test 19: A pressure of about 85 psi was applied to give a 45 psi pressure differential on the 8-5/8 in. x 5-1/2 in. annulus for 30 minutes, and the pressures on all string gauges were recorded after every minute. There was essentially no change in pressure on either the tubing or intermediate annulus, during the 30 minute period of holding the 45 psi pressure differential on the outer annulus, see Appendix 6.

Test 20; 21: The test was repeated for initial pressure differentials of 60 and 85 psi. For the 60 psi initial pressure differential (outer annulus held constant at 108 psi), there was no change in pressure on the tubing whilst a gradual 18 psi increase in pressure was observed on the intermediate annulus, see Fig. 40. For the 85 psi initial pressure differential (outer annulus held constant at 124 psi), there was an immediate increase of 34 psi followed by a gradual increase of another 22 psi in pressure on the intermediate annulus. Simultaneously, the tubing pressure was essentially constant until 14 minutes after the annulus pressure was applied. At that time, the increasing pressure on the intermediate annulus caused a differential pressure on the tubing of 75 psi, and the tubing pressure began increasing, eventually by about 40 psi, see Fig. 41 and Appendix 6.

Test 22: Comparative tests of manual pulsation were conducted using the pneumatic pump to simulate pulsation on the 8-5/8 in. x 5-1/2 in. annulus. After 20 hours of static time, a pulse magnitude of 85 psi and a 120/120-second cycle was simulated. There was appreciable response in both tubing and intermediate annulus after four pulses and thereafter, see Appendix 7 and Fig. 42.

Test 23: The pulsation test was repeated with a pulse magnitude of 45 psi and a 60/60-second cycle. There was no change in both tubing and intermediate annulus after 20 pulses, see Appendix 7.

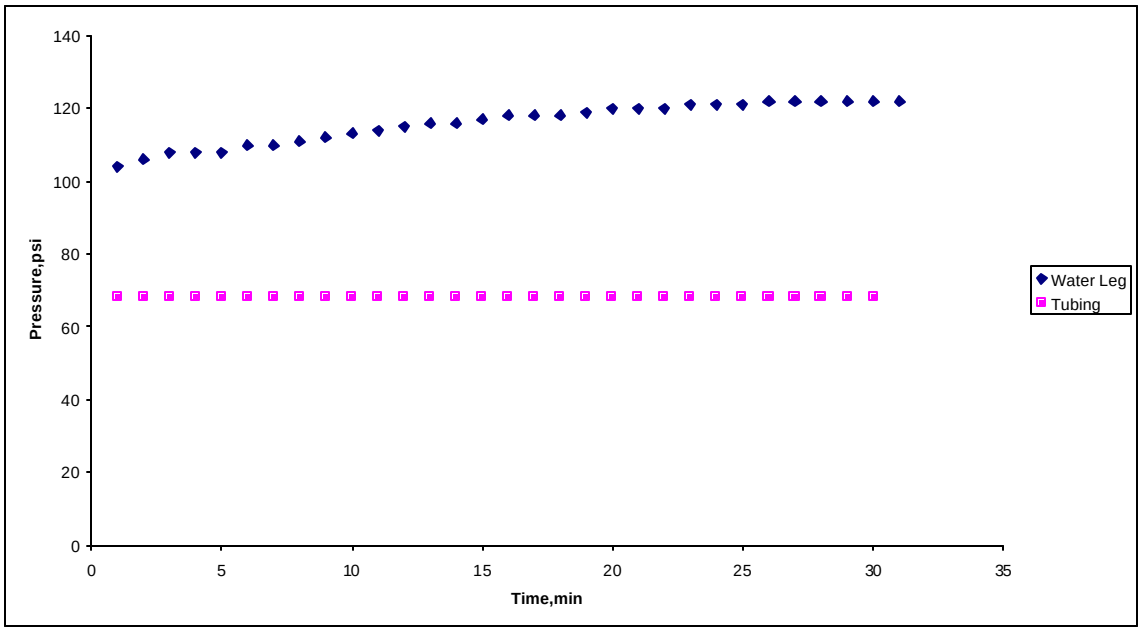

Figure 40. Test 20- Effect of applying 60 psi initial pressure differential on outer annulus

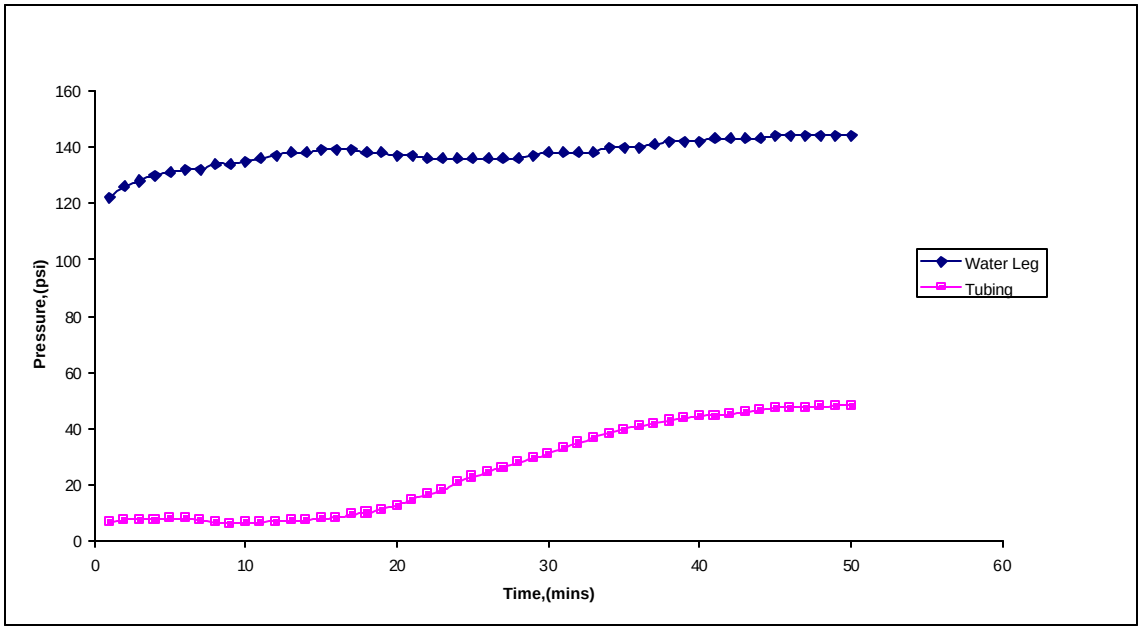

Figure 41. Test 21-Effect of applying 85 psi initial pressure differential on outer annulus after 18 hours static

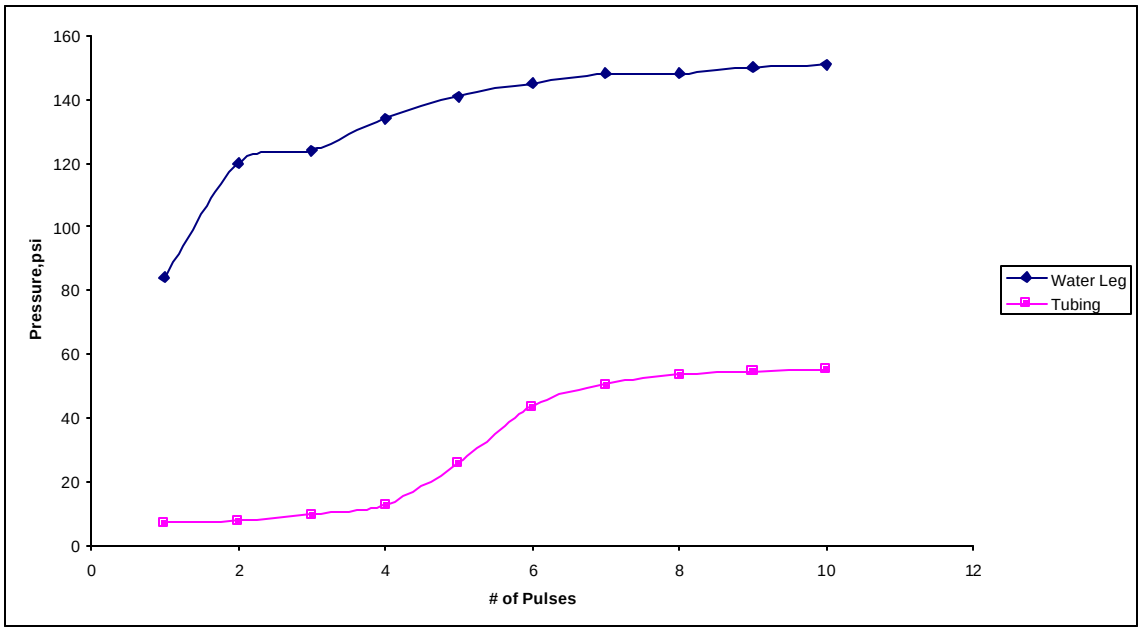

Figure 42. Test 22-Effect of 85 psi pulses (2/2) minutes cycle on outer annulus after 20 hours static

6.6 Analysis of Results

6.6.1 Effect of Yield Stress on Pressure Transmission

The yield stress of a fluid is defined as the minimum stress required to move (or permanently deform) the fluid. Below the yield stress, the fluid acts as an elastic solid and above the yield stress the fluid flows with a plastic viscosity, (Clark P.E et al, 1990). In our experiments, the yield stress was estimated from the 3 and 6 rpm dial readings of the Fann 35 viscometer using Equation 22.

$$YS = q_3 - (q_6 - q_3) \quad \text{.....(22)}$$

where:
YS – yield stress
θ_3 – 3 rpm dial reading
θ_6 – 6 rpm dial reading

From Test 1, it was observed that a pressure increase of 50 psi above the base pressure on the 8-5/8 x 5-1/2 in. annulus caused a response of 15 psi on the intermediate annulus. This indicated that pressure communication between the outer and intermediate annulus was established most likely as a result of the gels being broken in the outer annulus by the applied pressure differential. No response was observed on the tubing until the pressure was increased to 70 psi above the base pressure, see Appendix 1 and Fig. 29. This was also evident in the pulsation test. In pulsation Test 3, when a pulse of 60 psi was applied on the 8-5/8 x 5-1/2 in. annulus, a response of 12 psi was observed on the intermediate annulus after 5 pulses while no change was observed on the tubing pressure. The pressure on the intermediate annulus increased approximately 27 psi over its initial value in response to repeated pulsation of up to 20 pulses.

See Appendix 2 and Fig. 30. The pulse magnitude of 60 psi was not strong enough to affect any response in the tubing. A similar trend was observed in pulsation Test 5, when pulses of 66 psi were applied to the outer annulus. The pressure on the intermediate annulus increased by about 9 psi over its initial value after 20 pulses, while no response was observed on the tubing.

Using eq. 21, the estimated pressure differential required to establish communication on the outer annulus and tubing based on the gel strength of 125lbs/100 sq ft is 488 and 704 psi respectively. As noted previously, these pressures are much higher than the actual pressures measured when establishing communication in these tests. However, if the yield stress of 12 lbs/100 sq ft is used as the estimate of the wall stress in this equation, the estimated differential pressures are 47 and 68 psi respectively.

6.6.1.1 Minimum Pressure Differential to Establish Communication in Outer Annulus

It can be seen from the above discussion that a step pressure of 50 psi and pulse magnitude of 60 and 66 psi was enough to cause response in the intermediate annulus. These pressures are all greater than 47 psi that was the estimated pressure differential required to establish communication on the outer annulus based on yield stress. However, these pressures were not high enough to initiate communication with the tubing, which required an estimated pressure differential of 68 psi or greater. In Test 19, when a pressure differential of 45 psi was applied and held for 30 minutes on the outer annulus, there was no response on either the tubing or the intermediate annulus. Also, in Test 23, when a simulated manual pulsation of 45 psi pulse magnitude was applied on the outer annulus, there was no response on either the tubing or the intermediate annulus after 20 pulses. Therefore the 47 psi estimate based on yield stress is appropriate for the minimum pressure differential required to initiate communication through the outer annulus.

6.6.1.2 Minimum Pressure Differential to Establish Communication in Tubing

In Test 1, when the pressure on the outer annulus was increased to 70 psi above the base pressure, a response of 5 psi was observed on the tubing. As noted in the discussion of that test, the differential pressures on the tubing were inexplicably lower than in most subsequent tests. In pulsation Test 6, a maximum differential pressure of 61 psi was applied with a weak indication of communication to the surface through the tubing. Tests where less than 60 psi differential was applied to the tubing generally resulted in no communication. However, in pulsation Test 7, a pulse magnitude of 85 psi effected response in both the intermediate annulus and after a differential pressure of 63 psi occurred, in the tubing.

In Test 21, when a pressure differential of 85 psi was applied on the outer annulus, there was an immediate increase of 34 psi followed by a gradual increase of another 22 psi in pressure on the intermediate annulus. The tubing pressure was essentially constant until 14 minutes after the annulus pressure was applied. The maximum pressure differential observed on the tubing was 75 psi as communication was established. The tubing pressure then began increasing, eventually by about 40 psi, see Fig. 41 and Appendix 6. Likewise in Test 22, with 85 psi pulsation, a maximum pressure differential of 65 psi was required to establish communication. Therefore the 68 psi estimate based on yield stress seems reasonable as the minimum pressure differential required to establish pressure communication through the tubing.

6.6.1.3 Summary of Yield Stress Analysis

It can be inferred from the results of the pressure transmission and pulsation tests that significantly less pressure differential is required to break circulation or re-establish pressure

communication versus the pressure predicted based on gel strengths using eq. 21. We can also deduce from the above analysis that the pressure applied in both pulsation (pulse size or amplitude) and static pressure tests has a significant effect on pressure transmission. The pulse size required to re-establish communication should be at least equal to the pressure differential estimated by eq. 21, using yield stress in place of gel strength.

6.6.2 Effect of Pulse Frequency and Pulse Proportioning

Effectiveness of pulse frequency can be observed in pulsation Tests 6, 7, and 8. In all three tests, the same pulse magnitude of 85 psi was applied on the outer annulus but with different frequencies, and therefore periods, and proportioning. In Test 6, a 20/20 second cycle was used, and there was no response on the tubing after 10 pulses. An increase of only 2 psi was observed on the tubing after additional 10 pulses. In Test 7, a 40/40-second cycle was used, and a response of 14 psi was observed on the tubing after 10 pulses. In Test 8, an 80/20-second cycle was used giving both a longer period and different proportioning. A response of 20 psi was observed on the tubing after 10 pulses. The even longer 100/50 second cycle used in Test 9 resulted in no substantial improvement versus Test 8. From these comparisons, we can conclude that the longer pulse period of 80/20-second cycle appeared to be the most effective for the fluid properties and well geometry in these tests.

6.6.3 Effect of Shear-Sensitive Fluid Properties

The basic influence of yield stress on pressure transmission in a fluid column was described in Section 6.6.1. The gel strength of both cement and the cement-like slurry increases with time, and gel strength is generally believed to dominate pressure transmission in static cement columns. Therefore tests were conducted at various static times with the resultant different gel strengths. Tests 14, 15, 16, 17, and 18 were conducted for static times ranging from 10 minutes to 67 hours.

A summary of fluid properties, versus the measured pressure differential as pressure communication was established, can be seen in Table 25. Comparing the results in Table 25 with the estimates in Table 24 shows that the measured pressures to re-establish communication are more closely linked to yield stress rather than to gel strength, as concluded in Section 6.6.1. However, the maximum pressure differential required to re-establish pressure communication in a column of cement-like slurry increased with time as the gel strength increased, see Table 25 and Fig. 39. This confirms that gel strength, as well as yield stress, influences pressure transmission.

The effect of gel strength seems evident in Fig. 39-A. The peak differential pressures were greater in this test with the fluid after it had developed a high gel strength than in test with lower gel strengths. The reduction in differential pressure after the peaks seems to confirm that the peak is due to the pressure required to break the gel strength. However, the peak is not as large as if the gel strength of the entire column had to be broken simultaneously as presumed in the original form of eq. 21 and shown in Table 24. In fact, Fig. 39-A clearly shows that the gels in the annulus are broken before the gels in the tubing and that almost no pressure was transmitted to the tubing until the gels in the annulus were broken. After the gels are broken, pressure transmission is still suppressed, apparently by the yield stress of the fluid. This results in a residual differential pressure opposing pressure transmission even after the gel is broken.

The process of restoring pressure transmission through a cement column can be thought of being something like unzipping. A pressure change at one end of a cement column is only transmitted to the other end when the gel strength is broken or “unzipped” over the full length of the column, then yield stress still opposes pressure transmission. Therefore the increase in both

of these parameters that occurs after cement placement would suppress the transmission of hydrostatic pressure downhole.

6.6.4 Evaluation of Pulsation Versus Applying Constant Pressure

The effect of pulsation versus single static pressure on a column of gelled fluid can be evaluated by comparing Tests 21 and 22. In both tests, a pressure of 85 psi was applied on the outer annulus. The pulsation Test 22 proved to be more effective than single static pressure in Test 21 for restoring pressure communication through the gelled cement-like fluid. This can be seen from Figs. 41 and 42. Even though the pulse magnitude of 85 psi generated a response in both the single static pulse and the pulsation test, it took only two pulses (8 minutes) to get a 2 psi response in the pulsation test, whilst a 2 psi response in the static test was observed after 15 minutes. Secondly, the magnitudes of the response at all points in time in the pulsation test are greater than those in the single static pulse test, see Fig. 43.

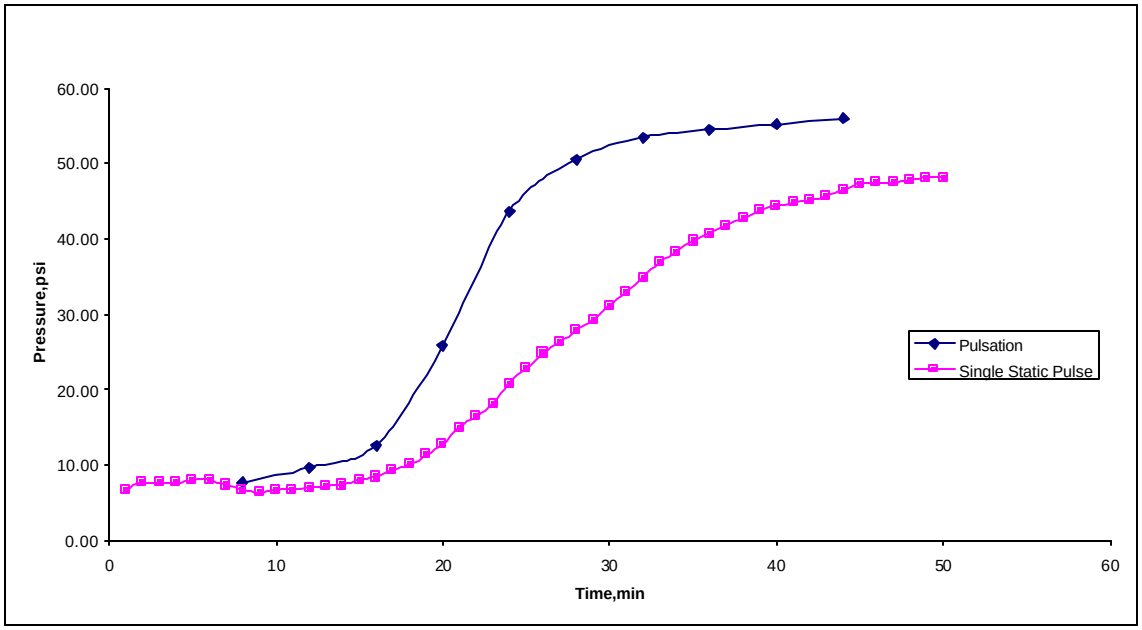

Figure 43. Pressure response observed on tubing for 85 psi pulse magnitude

The effectiveness of pulsation in restoring pressure transmission is also demonstrated in Test 11. In this test, a pulse magnitude of 110 psi and 60/40 second cycle was applied on the outer annulus. The pressure on the intermediate annulus increased from 67 psi to 156 psi while the response on the tubing increased from 4 to 70 psi after 10 pulses, see Appendix 2. Only 40 psi of the applied pulse amplitude was not transmitted to the tubing versus 80 to 90 psi not transmitted in Tests 16 and 17. Therefore pulsation appears to transmit pressure more effectively than a ramp pressure increase assuming the smaller pressure losses in Test 1 were an anomaly. In addition, this kind of effect should be even greater in cements where movement due to pulsation should retard the increase of yield stress with time. Consequently, pressure pulsation seems to give more, or at least faster, restoration of pressure transmission than application of a constant pressure of the same amplitude.

6.6.5 Release of Stored Energy When Gel is Broken

Some evidence of releasing stored energy or trapped pressure was observed in the pressure transmission tests. In the pressurization Test 13, the pressure response on the intermediate annulus increased from 66 psi to 98 psi, when the pressure on the tubing was increased from 110 psi to 120 psi, a 10 psi pressure increment. A subsequent 10 psi increment raised the intermediate annulus pressure by 28 psi, see Table 26 and Fig. 44.

Table 26. Pressurization on tubing-Test 13

Surface Tubing Pressure,psi	Increment in tubing pressure,psi	Intermediate Annulus pressure,psi	Magnitude of incremental response in intermediate annulus presure, psi
80	10	58	0
90	10	60	2
100	10	62	2
110	10	66	4
120	**10**	**98**	**32**
130	**10**	**126**	**28**

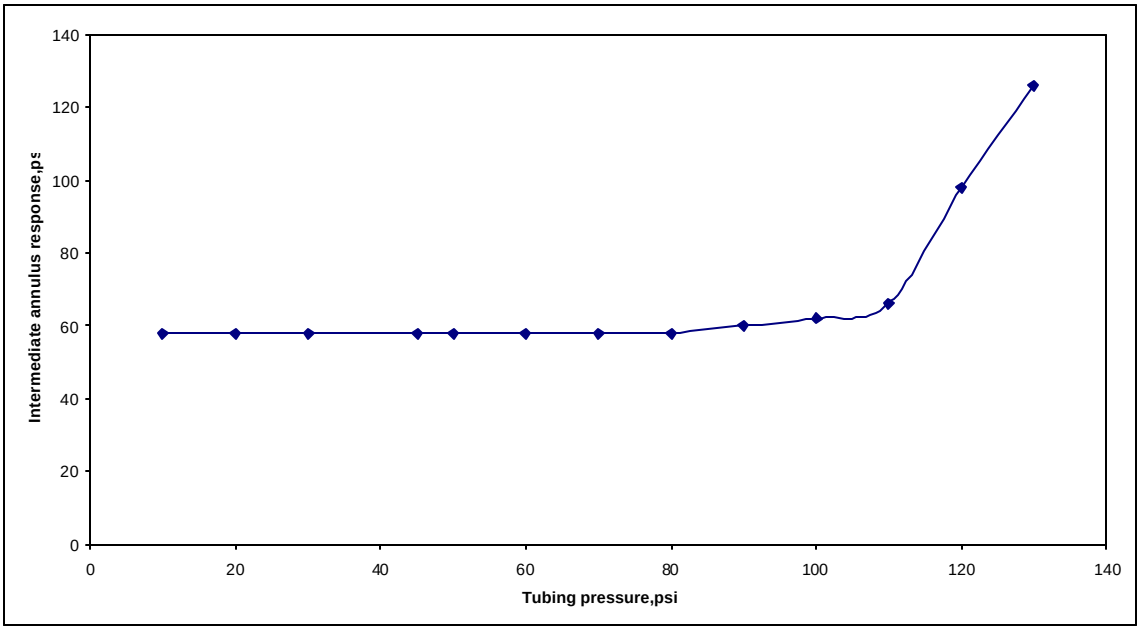

Figure 44. Release of stored energy when pressurizing tubing

The pressure transmission tests with the pressure applied to the outer annulus in Tests 14 to 18 generally have a similar, common trend behavior. Moreover, an apparent gelation effect is quite noticeable in the tubing response in Tests 14 and 18, see Figs. 34 and 38. These tests were conducted at low pumping rates after long static periods, see Table 27. Stored energy, pressure trapped by the high gel strengths was partially transmitted to the tubing in both tests when the gel was broken. In Test 14, the tubing pressure increased from 12 to 58 psi and a further increase of 22 psi for only a 6 psi pressure increment on the outer annulus. Similarly, in Test 18, the tubing pressure increased from 73 to 132 psi, that is an increase of about 59 psi, for only an increase of 20 psi on the outer annulus. Tests while bleeding pressure would be more analogous to the loss of bottomhole pressure in a cement column. However, our bleeding tests were generally done too

soon after pressurization to observe a large impact of gel strength. Nevertheless, breaking gel strength in a column should release the pressure that was held by the gel strength to be transmitted.

Table 27. Pumping rate for various static time

Static Time	Test No.	Total volume of water pumped	Total pumping time	Average pumping rate
		cc	mins	cc/min
10 mins.	17	29570	17	1739
2 hours	16	27890	30	930
20 hours	14	37830	70	540
67 hours	18	25230	75	336

6.7 Summary of Observations

- Significantly less differential pressure is required to break circulation or re-establish pressure communication than predicted by the conventionally accepted theory as embodied in eq. 21. (See Section 6.6.1.)
- Pressure required to break circulation is much more closely linked to the yield stress than to the gel strength of the slurry. However, the maximum pressure differential required to re-establish pressure communication in a fluid column does increase gradually with time as the gel strength increases. Therefore early initiation of pulsation should be advantageous for maximizing the depth of pressure transmission. (See Section 6.6.1. and 6.6.3.) Additional research is required to investigate these time sensitive effects for cements.
- The amplitude of the pressure pulse has a significant effect on pressure transmission. For pulsation to be effective, the pulse amplitude should generally be at least equal to the pressure predicted by eq. 21, as revised to use yield stress in place of gel strength. (See Section 6.6.1.)
- Pulsation is a faster, and therefore presumably more effective, means of re-establishing pressure transmission than a single static pressure pulse. (See Section 6.6.4.)
- Pulsation should have an advantage versus other methods of maintaining hydrostatic pressure by causing fluid movement that retards progressive development of yield stress and gel strength of the cement slurry over time. (See Section 6.6.4.)
- The period, or frequency, of pressure pulsation and the duration of the high pressure sub-period apparently influence the degree of pressure transmission achieved. This observation requires confirmation with more carefully controlled experiments. (See Section 6.6.2.)

CONCLUSIONS

1. The mechanism of flow after cementing has been extensively studied for the past 20 years. A hydrostatic pressure loss after cement placement has been identified as the primary reason for fluid migration outside wells. A well with progressive pressure loss becomes underbalanced, which results in formation fluid entry and migration.

2. Laboratory experiments and field tests indicate that cement slurry vibration is an effective method of cement fludization and preventing the loss of hydrostatic pressure. However, most of the techniques have been only demonstrated with no commercial use. Size of equipment needed to vibrate a long and heavy string of casing and cost of downhole vibrating devices rendered the technology impractical in field operations.

3. A simple analytical static model - developed in this research - relates the pressure pulse amplitude to the entire distribution of pressure in the cement column during and after the treatment. The static model includes basic phenomena of the process and provides insight of the process mechanism that can be summarized as follows:
    - The model reveals that the bottom part of the cement column may remain unaffected by the treatment. Also, the model provides an analytical tool for designing the desired pressure amplitudes that should be increased with time;
    - The model provides a theoretical proof of the behavior observed in the field experiments involving amplification of the top pressure pulse with depth. Moreover, the model suggests that the pressure pulse amplifying effect will diminish below a certain critical depth.
4. Cement slurries were tested in this study to determine the effect of continuous shearing on slurry gelation. The experiments showed that continuous shearing at 3 rpm, the lowest speed available with the Fann 35 viscometer, was enough to maintain the liquidity of the cement sample. Therefore, in this work shearing rate equivalent to 3 rpm was chosen as the minimum shearing rate to maintain liquidity of cement. This shearing rate did not appear to be a function of time and reached values between 57 and 116 s^{-1} depending on the plastic viscosity and yield point values of cement. It was then concluded that as low a shearing rate as 116 s^{-1} may be enough to prevent gelation of setting cement.

5. Compressibility of cement slurries was tested in this study to determine its correlatioin with the slurry gelation process. The results show little change in the cement compressibility over the test period. The result implies that the compressibility of the products of chemical reactions is of the same magnitude as the compressibility of the components. Thus, we conclude that during the transition time, cement compressibility remains a constant component of the annular compressibility of the wellbore.

6. A dynamic model of pressure wave propagation in Bingham plastic fluid was developed and used for parametric study of the TCP process and identification of best treatment strategy. The model shows that the pressure wave is attenuated mostly due the effects of plastic viscosity, yield point and size of the well annulus. The most disadvantageous conditions for wave propagation is the combination of high - yield point cement slurry in a small annulus.

1.

7. Theoretical computations show patterns of displacement amplitude change at the cement top during TCP. Thickening of cement slurry results in the increase of yield point and

plastic viscosity that, in turn, reduces the displacement amplitude throughout the cement column. As the thickening process may not be uniform at all depths, the pattern of top cement displacement may also differ. Thus, monitoring of the top cement displacement during the CP treatments may provide important information on cement quality.

7. A full-scale experimental study has been conducted in this project to validate the underlying concepts for cement pulsation and the factors influencing its effectiveness. The study employed full-size wells and cement-like slurries simulating early gelation and rheology of oilwell cements. The results from the study showed that:
   - Top pulsation is a faster, and therefore presumably more effective, means of re-establishing pressure transmission than a single static pressure pulse;
   - Pulsation should have an advantage versus other methods of maintaining hydrostatic pressure by causing fluid movement that retards progressive development of yield stress and gel strength of the cement slurry over time;
   - Early initiation of top pulsation should be advantageous for maximizing the depth of pressure transmission. The maximum pressure differential required to re-establish pressure communication in a stagnant fluid column does increases gradually with time as the gel strength increases.

8. New research is needed to develop TCP technology for field deployment. The research should address laboratory testing of cements to find time-dependent rheology that is critical for TCP design. Also, addressed should be the effect of pulsation on compressive strength, permeability, and bonding properties of cement in the well annulus. Moreover, monitoring of top cement amplitude and motion during TCP should be evaluated as a potential new logging tool for cement quality assessment.

BIBLIOGRAPHY

Specifications for Materials and Testing for Well Cements. API Spec 10, American Petroleum Institute, Dallas (1988).

Banfill, P. F. G. "Viscometric Studies of Cement Pastes Containing Superplasticizers." *Magazine of Concrete Research* 33, no. 114 (March1981): 40.

Banfill, P. F. G., and D. C. Saunders. "On the Viscometric Examination of Cement Pastes." *Cement and Concrete Research* 11, no. 3 (1981): 363.

Binder R. C. *Advanced Fluid Dynamics and Fluid Machinery*. New York: Prentice Hall, 1951.

Bodine, A. G., and Y. N. Gregory. "Sonic Cementing. " U.S. Patent 4,640,360 (Feb. 3, 1987).

Bourgoyne, A. T. Jr. et al. *Applied Drilling Engineering.* Society of Petroleum Engineers, Richardson, TX (1986): 154.

Carter, G., and K. Slagle. "A Study of Completion Practices to Minimize Gas Communication." SPE 3164. Central Plains Regional Meeting, Society of Petroleum Engineers of AIME, Amarillo, TX (Nov. 16 -17, 1970).

Carter, G., C. Cook, and L. Snelson. "Cementing Research in Directional Gas Well Completions." SPE 4313. Second Annual European Meeting, Society of Petroleum Engineers of AIME, London, England (Apr. 2-3, 1973).

Chou, T. W., L. V. McIntire, U. R. Kunze, and C. E. Cooke. "The Rheological Properties of Cement Slurries: Effects of Vibration, Hydration Conditions and Additives." SPE 13836 (1988).

Christian, W. W., J. Chatterji, and G. Ostroot. “Gas Leakage in Primary Cementing: A Field Study and Laboratory Investigation.” SPE 5517. 50th Annual Fall Meeting, Society of Petroleum Engineers of AIME, Dallas, TX (Sept. 28 - Oct. 1, 1975).

Clark, P. E., Sundaram, L., and Balakrishnan, M. "Yield Points in Oilfield Cement Slurries." SPE 21279. SPE Eastern Regional Meeting, Columbus, OH (October 31 - November 2, 1990).

Cooke C. E. Jr., M. P. Kluck, and R. Medrano. “Field Measurements of Annular Pressure and Temperature During Primary Cementing.” SPE 11206 (1982).

Cooke, C. E. Jr. “Method for Preventing Annular Fluid Flow.” U.S. Patent 4,407,365 (Oct. 4, 1983).

Cooke, C. E., O. J. Gonzalez, and D. J. Broussard. “Primary Cementing Improvement by Casing Vibration During Cementing Casing Time.” SPE 14199 (1988).

Haberman, Y. P., M. Delestatius, and D. G. Brace. “Method and Apparatus to Improve the Displacement of Drilling Fluids by Cement Slurries.” U.S. Patent 5,377,753 (Jan. 3, 1995).

Haberman, Y. P. “Sealing Gas Zones By Vibrating Cement Slurries.” *Gas Tips*. GRI (Spring 1996):19-23

Haberman, J. P. and S. L. Wolhart. “Reciprocating Cement Slurries after Placement by Applying Pressure in the Annulus.” SPE 37619 (1997).

Hartog, J. J., D. R. Davies, and R. B. Stewart. “An Integrated Approach for Successful Primary Cementations.” *JPT* (September 1983).

Keller, S. R. “Oscillatory Flow Method for Improved Well Cementing.” U.S. Patent 4,548,271 (Oct. 22, 1985).

Manowski W. M. “Design Method for Top Cement Pulsation to Prevent Flow after Cementing.” M.S. Thesis, Louisiana State University, 1997.

Rankin, R. E., and K. T. Rankin. “Apparatus and Method for Vibrating a Casing String during Cementing.” U.S. Patent 5,152,342 (Oct. 6, 1992).

Raymond, L. R. “Temperature Distribution in a Circulating Drilling Fluid.” *JPT* (March 1969):333.

Sabins, F. L., J. M. Tinsley, and D. L. Sutton. “Transition Time of Cement Slurries between the Fluid and Set State.” SPE 9285 (1988).

Schlumberger. *Well Cementing*. Nelson, E.B. ed. Educational Services, 1990.

Solum, K.W. et al. “Method and Apparatus for Vibrating and Cementing a Well Casing.” U.S. Patent 3,557,875 (Jan. 26, 1971).

Streeter V. L. and B. E. Wylie. *Hydraulic Transients.* McGraw-Hill, 1967.

Sutton, D. L., and U. M. Ravi. “New Method for Determining Downhole Properties That Affect Gas Migration and Annular Sealing.” SPE 19520 (1989).

Sutton, D. L., and U. M. Ravi. “Low-Rate Pipe Movement During Cement Gelation to Control Gas Migration and Improve Cement Bond.” SPE 22776 (1991).

Winbow, G. A. “Method for Preventing Annular Fluid Flow Using Tube Waves.” U.S. Patent 5,361,837 (Nov. 8, 1994).